1. REPORT NO.	2. GOVERNMENT ACCESSION NO.	3. RECIPIENT'S CATALOG NO.
WA-RD 704.1		

4. TITLE AND SUBTITLE	5. REPORT DATE
DYNAMIC MODULUS TEST – LABORATORY INVESTIGATION AND FUTURE IMPLEMENTATION IN THE STATE OF WASHINGTON	December 2007
	6. PERFORMING ORGANIZATION CODE
7. AUTHOR(S)	8. PERFORMING ORGANIZATION REPORT NO.
Laith Tashman, Muthukumaran A Elangovan	
9. PERFORMING ORGANIZATION NAME AND ADDRESS	10. WORK UNIT NO.
Washington State Transportation Center (TRAC) University of Washington, Box 354802 University District Building; 1107 NE 45th Street, Suite 535 Seattle, Washington 98105-4631	11. CONTRACT OR GRANT NO.
12. SPONSORING AGENCY NAME AND ADDRESS	13. TYPE OF REPORT AND PERIOD COVERED
Research Office Washington State Department of Transportation Transportation Building, MS 47372 Olympia, Washington 98504-7372	Final Research Report
	14. SPONSORING AGENCY CODE

15. SUPPLEMENTARY NOTES

This study was conducted in cooperation with the U.S. Department of Transportation, Federal Highway Administration.

16. ABSTRACT

A database of dynamic modulus values for typical Superpave mixes widely used in the state of Washington was developed and used to investigate the sensitivity of the dynamic modulus to aggregate gradation. Seven JMF (job mix formula) mixes were selected for the study. Percent passing sieve #200 of these mixes were changed by ± 2% to prepare additional mixes referred to as 'modified mixes'. Statistical analysis showed that using different JMF mixes significantly affected the dynamic modulus. This was not the case when modifying the JMF by changing the percent passing #200. A simple evaluation of the prediction accuracy of the 2002 Mechanistic-Empirical Pavement Design Guide (MEPDG) was conducted in which the measured dynamic modulus was used as a key input parameter to predict pavement distresses. Level 1 and Level 3 predictions of rutting, longitudinal cracking, alligator cracking, and IRI were compared with the field performance data. The Design Guide predicted IRI and alligator cracking reasonably well. The predicted rutting of the JMF mixes agreed well with the dynamic modulus trend. It was found that the ±2% change in the passing #200 aggregate gradation did not affect the predicted distress significantly.

17. KEY WORDS	18. DISTRIBUTION STATEMENT
dynamic modulus, dynamic modulus sensitivity, aggregate gradation, MEPDG, predicted distress,	No restrictions. This document is available to the public through the National Technical Information Service, Springfield, VA 22616

19. SECURITY CLASSIF. (of this report)	20. SECURITY CLASSIF. (of this page)	21. NO. OF PAGES	22. PRICE
None	None	48	

LIST OF FIGURES

LIST OF TABLES

DISCLAIMER

The contents of this report reflect the views of the authors, who are responsible for the facts and the accuracy of the data presented herein. The contents do not necessarily reflect the official views or policies of the Washington State Department of Transportation or the Federal Highway Administration. This report does not constitute a standard, specification, or regulation.

DYNAMIC MODULUS TEST – LABORATORY INVESTIGATION AND FUTURE IMPLEMENTATION IN THE STATE OF WASHINGTON

Introduction

There is currently a national effort to implement performance tests as part of the Superpave mix design criteria for Hot Mix Asphalt (HMA). Recent findings of the National Cooperative Highway Research Program (NCHRP) emphasized the importance of the dynamic modulus test as a "Simple Performance Test" that correlates with the performance of HMA and complements the mix design criteria. The dynamic modulus is considered a key material characterization parameter in the design input of the *2002 Guide for Mechanistic-Empirical Design of New and Rehabilitated Pavements Structures* (MEPDG), which has been recently released by NCHRP (NCHRP Project 1-37A) for investigation. Washington State Department of Transportation (WSDOT) is in the process of implementing the Superpave technology in their standard specifications for the design and construction of HMA. The implementation of the Superpave technology in the State of Washington and the release of the MEPDG make it urgent to establish a database of dynamic modulus values for HMA mixes that are widely used in the State of Washington for the purpose of evaluation and implementation and for future studies.

The primary objective of this study is to develop a database of dynamic modulus values of typical Superpave HMA mixes that are widely used in the State of Washington. The database will be used to investigate the sensitivity of the dynamic modulus to HMA mix properties and its relationship to field performance. It will also be used to evaluate the MEPDG.

Dynamic Modulus Test

The dynamic modulus is a complex number defining the stress strain relationship of linear viscoelastic materials under a continuous sinusoidal loading. Mathematically, the dynamic modulus is the ratio of the peak dynamic stress (σ_o) to the peak recoverable axial strain (ε_o). The viscous behavior of HMA is indicated by the phase angle (Φ), which is the angle by which ε_o lags behind σ_o. The closer is the phase angle to 90°, the more viscous is the material.

$$|E^*| = \frac{\sigma_o}{\varepsilon_o} \tag{1}$$

The dynamic modulus is a function of HMA mix properties and non-material properties including the test temperature, frequency, and possibly specimen geometry (specimen height-to-diameter ratio). The 2002 design guide advocates the use of a ratio of less than two. Vivek et al. (2006) evaluated the effect of height-to-diameter ratio on the accuracy of the results and the significance of end friction reducing (EFR) membranes on dynamic modulus. They reported that specimens with a diameter of 152 mm instead of the standard 102 mm provided more consistent results, especially when the ratio was less than two. The accuracy of the measured dynamic modulus increased and the variability was reduced by using EFR membranes. Christopher et al. (2006) examined the effects of testing history and method of specimen preparation (sawed/cored

or compacted) on the dynamic modulus. They concluded that the two factors do not affect the dynamic modulus significantly.

The dynamic modulus test is still in the implementation stages in many states. Prior to implementing the test, it is important to carry out evaluation studies for local conditions to have first-hand information on the dynamic modulus values of commonly used mixes. Shah et al. (2005) measured the dynamic modulus on eleven mixes commonly used in the North Carolina region and reported that it was sensitive to binder content; higher sensitivity for modified binder. The findings from the study were used for providing feedback on the implementation of the test method. Zhou et al. (2003) used field pavement conditions to validate the dynamic modulus test and the associated parameter, $E^*/\sin\phi$, for implementing the test in day-to-day Superpave design practice. Their results clearly showed that the dynamic modulus test and the $E^*/\sin\phi$ can distinguish between good and poor mixtures.

Mechanistic Empirical Guide

The *2002 Guide for Mechanistic-Empirical Design of New and Rehabilitated Pavement Structures* (MEPDG) is the new guide for pavement design. All design guides preceding the 2002 MEPDG were based on limited empirical equations developed by the AASHTO Road Test in the late 1950's. The significant changes in the materials, trucks and truck volumes, and construction techniques created the need for a more robust mechanistic empirical design procedure that also takes into account the climatic effects on the pavement performance, can predict important types of distresses, and capable of adapting to new conditions. The guide utilizes existing mechanistic models and current pavement design procedures. The impact of climate and aging on material properties was incorporated in the form of biweekly and monthly iterative predictions for the entire design life of the pavement. The selected mechanistic-based distress prediction models were calibrated comprehensively until a reasonable prediction of pavement performance was achieved. Finally, the complex models and design concepts were incorporated into a user-friendly software package. Improvisations to the design procedure and software can be made over time in a piecewise manner to any of the component models and incorporate them in the procedure after recalibration.

The MEPDG software can be used for designing new/rehabilitated, flexible/rigid pavements, which requires a comprehensive list of inputs. An important aspect of the MEDPG is that it provides three hierarchical levels of design inputs, namely Level 1, Level 2, and Level 3. Level 1 input provides the highest level of accuracy and would be used for heavily trafficked pavements, or where safety and economic considerations for an early failure are a concern. Level 2 inputs provide an intermediate level of accuracy and could be used when resources or testing equipments are not available. These are typically one of the following: user-selected possibly from an agency database, or derived from limited testing program, or estimated through correlations. Level 3 inputs provide the lowest level of accuracy and might be used for design where there are minimal consequences of early failure. These are typically one of the following: user-selected or typical averages for the region. The hierarchical input system was devised upon the premise that the design reliability should logically increase when the level of engineering effort used to obtain inputs is increased. This concept was validated only for the thermal fracture

module in the guide. The guide recommends the confirmation of this hypothesis for at least one major load-related distress, by which it will be illustrated that additional time and effort will result in a lower cost and better performance of the pavement. The guide classifies the inputs required for the design or analyzing a pavement into three major categories: traffic, climate, and materials. Another important aspect of the guide is the incorporation of the weather station driven Enhanced Climatic Integrated Model (EICM), used to model temperature and moisture within each pavement layer as well as the subgrade. It is integrated directly into the determination of the modulus of the pavement and subgrade.

Approximately one-hundred inputs are required for using the MEPDG. Apparently, the prediction accuracy of the models is not sensitive to all of the inputs. Therefore, it is important to investigate the crucial inputs that dominate the prediction accuracy of the models. Currently, research efforts are focused towards the investigation of the sensitivity of prediction accuracy to HMA material properties and traffic inputs, as well as the hierarchical level of inputs. Ali (2005) used laboratory measured material properties as inputs to investigate the influence of material type on pavement performance predicted by the MEPDG. The model reflected sensitivity to HMA mix type. However the dynamic modulus, estimated using predictive equations incorporated in the guide, was substantially different from the measured values, which resulted in underestimating the permanent deformation. The model lacked sensitivity towards the variations in unbound material. They recommended the use of nonlinear analysis to capture the real behavior of unbound materials. The study also recommended the use of measured dynamic modulus (Level 1) rather than predicted values (Level 2). Carvalho (2006) used Level 3 inputs to study the performance prediction of the MEPDG and observed that variations of HMA layer thickness had significant impact on performance prediction. However, the thickness of the base layer had little influence on fatigue cracking and permanent deformation. They recommended that a database of material property inputs be developed for routine design applications. Mohammad et al. (2006) evaluated the 2002 M-E design guide software by investigating the sensitivity of dynamic modulus to predict rutting. They reported that more research is needed to validate and calibrate the rutting model used in the M-E design guide. Hall and Beam (2005) performed a study to assess the relative sensitivity of the models used in the M-E design guide to inputs related to Portland cement concrete materials in the analysis of jointed plain concrete pavements (JPCP). Twenty-nine inputs were evaluated by analyzing a standard pavement section and changing the values of each input individually. The pavement distress models (cracking, faulting, and roughness) were not sensitive to seventeen of the twenty-nine inputs. All three models were sensitive to six of the twenty-nine inputs. Combinations of only one or two of the distress models were sensitive to six of the twenty-nine inputs.

The inputs to the MEPDG may be obtained using a mix of levels, such as HMA mix properties from Level 1, traffic data from Level 2, and subgrade properties from Level 3. This was supported by the study carried out by Nantung et al. (2005). They reported that combinations of design input levels, rather than using a single design input level, can yield more rational results. They also observed that, in the traffic load spectra, the default values in Level 3 design input are too general that design accuracy may not be achieved and at least a traffic design input from Level 2 must be used.

In the development of the guide, the LTPP database was used for the calibration-validation of the distress/smoothness models. As a result, the guide needs to be evaluated for local conditions before implementing in the routine design process. Ceylan et al (2005), in support of the MEPDG implementation initiatives in Iowa, conducted sensitivity studies using the MEPDG software to identify design inputs pertaining to both rigid and flexible pavements that are of particular sensitivity in Iowa. Based on the results, they categorized the inputs for longitudinal and transverse cracking, rutting, and roughness for Iowa as *extremely sensitive* and *sensitive to very sensitive*. Based on the results of the sensitivity analyses, they presented a strategic plan for implementing the MEPDG in Iowa. Uzan et al (2005) carried out a sensitivity study to determine the input variables for the MEPDG most important to the Texas Department of Transportation (TxDOT). They found that the models predicted rut depth adequately, whereas alligator cracking was slightly over-predicted, and inconsistent results were observed for longitudinal cracking. The observations from the sensitivity study were used for the implementation of the MEPDG into TxDOT's normal pavement design operations. Gramajo (2005) used the MEPDG software to predicted distress using field data from pavement sections in the Commonwealth of Virginia as inputs. The predicted distresses were higher than the distresses observed in the field. The study concluded that significant calibration and validation is required before M-E Design Guide can be implemented.

Table 1. Volumetrics of the selected mixes and asphalt binder properties

	Mix ID						
	5381	**5295**	**5192**	**5373**	**5627**	**5364**	**5408**
NMAS, mm	12.5	12.5	12.5	19	19	12.5	12.5
MAS, mm	19	19	19	25	25	19	19
Asphalt content, %	5.7	5.3	5.1	5.4	4.5	5.6	5.4
Aggregate content, %	94.3	94.7	94.9	94.6	95.5	94.4	94.6
VFA, %	73	74.5	72.8	72.8	70.8	70.8	73.3
VMA, %	15.2	16.6	14.6	14.6	13.9	13.9	14.9
G_{mm}	2.492	2.486	2.483	2.551	2.616	2.502	2.523
G_{mb}	2.267	2.262	2.260	2.321	2.381	2.277	2.296
Asphalt							
PG	58-22	70-22	64-22	70-28	64-28	58-22	64-28
Mixing temp, °C	136-141	154-159	153-158	160-171	160-168	136-141	157-162
Compaction temp, °C	133-138	145-150	142-147	138-149	138-149	133-138	146-151
G_b	1.0269	1.038	1.02	1.021	1.035	1.02	1.03

Methodology

Seven Superpave mixes that have been used in the construction of flexible pavements by WSDOT were selected such that the aggregates in the mix are of different types from different sources, and that documented field performance data are available for the pavements constructed using the selected mixes. Table A1.1 summarizes the pavement sections constructed using the selected mixes. The aggregate - source, type, and other properties are summarized in Table A1.2. Table 1 summarizes the volumetrics of the selected mixes as well as the asphalt information.

Table 2. Aggregate gradations of the mixes

Project	Mix	Sieve sizes (mm)											
		25	19	12.5	9.5	4.75	2.36	1.18	0.6	0.3	0.15	0.075	<0.075
	JMF	-	-	6	9	30	18	12	7	6	4	3	5
5381	LM	-	-	6.1	9.2	30.6	18.4	12.2	7.1	6.1	4.1	3.1	3.1
	UM	-	-	5.9	8.8	29.4	17.6	11.8	6.9	5.9	3.9	2.9	6.9
	JMF	-	-	3	13	30	21	11	7	5	4	1.2	4.8
5295	LM	-	-	3.1	13.3	30.6	21.4	11.2	7.1	5.1	4.1	1.2	2.9
	UM	-	-	2.9	12.7	29.4	20.6	10.8	6.9	4.9	3.9	1.2	3.2
	JMF	-	-	2	9	35	11	9	7	13	8	2	5
5192	LM	-	-	2.2	8.5	35.1	11.7	9.1	73	13.5	7.5	1.6	5.2
	UM	-	-	2.2	8.5	35.0	11.2	8.8	7.0	13.0	7.5	1.6	3.2
	JMF	1	4	16	8	23	18	9	6	5	3	2	5
5373	LM	1.0	4.1	16.3	8.2	23.5	18.4	9.2	6.1	5.1	3.1	1.9	5.2
	UM	1.0	3.9	15.7	7.8	22.5	17.6	8.8	5.9	4.9	2.9	1.0	4.1
	JMF	-	4	21	12	16	15	11	7	4	3	1	6
5627	LM	-	4.1	21.4	12.2	16.3	15.3	11.2	7.1	4.1	3.1	1.0	3.2
	UM	-	3.9	20.6	11.8	15.7	14.7	10.8	6.9	3.9	2.9	1.0	7.8
	JMF	-	-	6	16	23	17	14	7	6	3	3	5
5364	LM	-	-	6.1	16.3	23.5	17.3	14.3	7.1	6.1	3.1	3.1	3.1
	UM	-	-	5.9	15.7	22.5	16.7	13.7	6.9	5.9	2.9	2.9	6.9
	JMF	-	-	5	13	32	17	10	7	5	4	2	5
5408	LM	-	-	5.1	13.3	32.7	17.3	10.2	7.1	5.1	4.1	2.0	3.1
	UM	-	-	4.9	12.7	31.4	16.7	9.8	6.9	4.9	3.9	2.0	6.9

JMF – Job Mix Formula; LM – lower modified mix; UM – upper modified mix

To investigate the sensitivity of the dynamic modulus to HMA mix properties, aggregate gradation of the seven JMF mixes were modified. The amount of mineral filler (passing sieve #200) is commonly known to be affected during HMA plant operation, which could influence the volumetrics of a mix significantly. Therefore, aggregate gradations for the sensitivity study were modified mainly by increasing/decreasing the percent passing sieve #200. To simulate field conditions, aggregate gradation was varied as per WSDOT field tolerance limits, summarized in Table A1.3. A 'lower modified mix' and an 'upper modified mix' were prepared using each JMF mix. In the lower modified mixes the percent passing sieve #200 was reduced by 2% and in the upper modified mixes it was increased by 2% (i.e. 2% change in percent passing, e.g. 7% becomes 5% for the lower and 9% for the upper modified mix). This resulted in a substantial decrease in the amount of mineral filler in the lower modified mixes and vice versa for the upper modified mixes (25 to 40% by weight). All other sieve sizes were slightly increased for the lower modified mixes and slightly decreased for the upper modified mixes (approximately 2% change by weight) in order to maintain the same aggregate content as the job mix formula (JMF). The quantitative variations for all the mixes are summarized in Table A1.4. A total of twenty-one mixes were prepared and grouped into seven projects. Each project comprised of three mixes: one JMF mix, one lower modified mix, and one upper modified mix. The seven projects and the aggregate gradation of all the mixes are summarized in Table 2.

HMA specimens for laboratory testing were 100 mm in diameter and 150 mm in height. The specimens were cut and cored from gyratory specimens that were 150 mm in diameter and 170 mm in height. A Superpave Gyratory Compactor (SGC) was used for the compaction of gyratory specimens in accordance with the AASHTO T 312. According to the AASHTO TP 62-03 there is a 1.5 to 2.0 percent decrease in percent air voids when a specimen is cut and cored from a gyratory specimen. Therefore, the target air void content was 9% in the compacted SGC specimens in order to achieve an air void content of 7 ± 1.0 % in the test specimens. The bulk specific gravity and percent air voids in both gyratory and test specimens (cut and cored) were measured using the Corelok apparatus. The results are summarized in the Table A1.5. Two replicates for each mix were prepared, that is a total of 42 SGC specimens. Thereafter, the following tests were performed:

1) Dynamic modulus test (E* and ϕ) on the HMA test specimens in accordance with the AASHTO TP 62-03
2) Static creep test (flow time) on the HMA test specimens
3) Complex shear modulus (G* and δ) on the asphalt binders.

The test conditions for dynamic modulus and complex shear modulus test are summarized in Table A1.6. The static creep tests were conducted at 130 °F.

Dynamic Modulus Master Curves

Dynamic modulus master curves were developed in accordance with the procedure described in the MEPDG. Shift factors were computed using Eq. 2 (Eq. 2.2.16 in the guide) and a sigmoid function defined by Eq. 3 (Eq. 2.2.15 in the guide) was used for fitting the shifted E* data.

$$\log(t_r) = \log(t) - c[\log(\eta) - \log(\eta_{T_r})] \quad (2)$$

$$\log(E*) = \chi + \frac{\alpha}{1 + e^{\beta + \gamma[\log(t) - c(\log(\eta) - \log(\eta_{T_r}))]}} \quad (3)$$

where

E*	=	dynamic modulus, MPa
t_r	=	time of loading at the reference temperature
t	=	time of loading, sec
η	=	viscosity at temperature of interest, cP
η_{Tr}	=	viscosity at reference temperature, cP
α, β, χ, γ, c	=	mixture specific fitting parameters

$$\eta = \frac{G^*}{10}\left(\frac{1}{\sin\delta}\right)^{4.8628} \quad (4)$$

$$\log\log\eta = A + VTS\log(T_R) \quad (5)$$

where

G*	=	binder complex shear modulus, Pa
δ	=	binder phase angle, degrees
η	=	viscosity, cP
T_R	=	temperature in Rankine at which the viscosity was determined
A, VTS	=	regression parameters

The viscosity of asphalt is a necessary parameter for computing the shift factors. Eq. 4 (Equation 2.2.13) is a correlation between η, G*, and δ recommended by the MEPDG. It was used for computing viscosities of the asphalt binders used in the study. The G*, δ, and η are summarized in Table A2.1. In the recent version of the MEPDG software (version 1.000), it has been mandated to input E* at a temperature ranging between 0 and 20 °F. This temperature range is hard to achieve in the laboratory using the Simple Performance Tester currently available at the Washington Center for Asphalt Technology (WCAT). Therefore, E* values at 14°F was predicted using the sigmoid function in Eq. 3. Viscosity of the asphalt binders at this temperature was calculated using Eq. 5 (Equation 2.2.14 in the guide). At very low temperatures, the viscosity of asphalt tends to reach a plateau. According to the MEPDG, the viscosity of asphalt at very low temperatures must be limited to 2.70 x 10^{10} Poise (Refer to Part 2 Chapter 2 of the Guide). Considering this fact, while predicting the E* values at 14°F, the viscosity of asphalt was limited to 2.70 x 10^{10} Poise if the predicted viscosity exceeded this value.

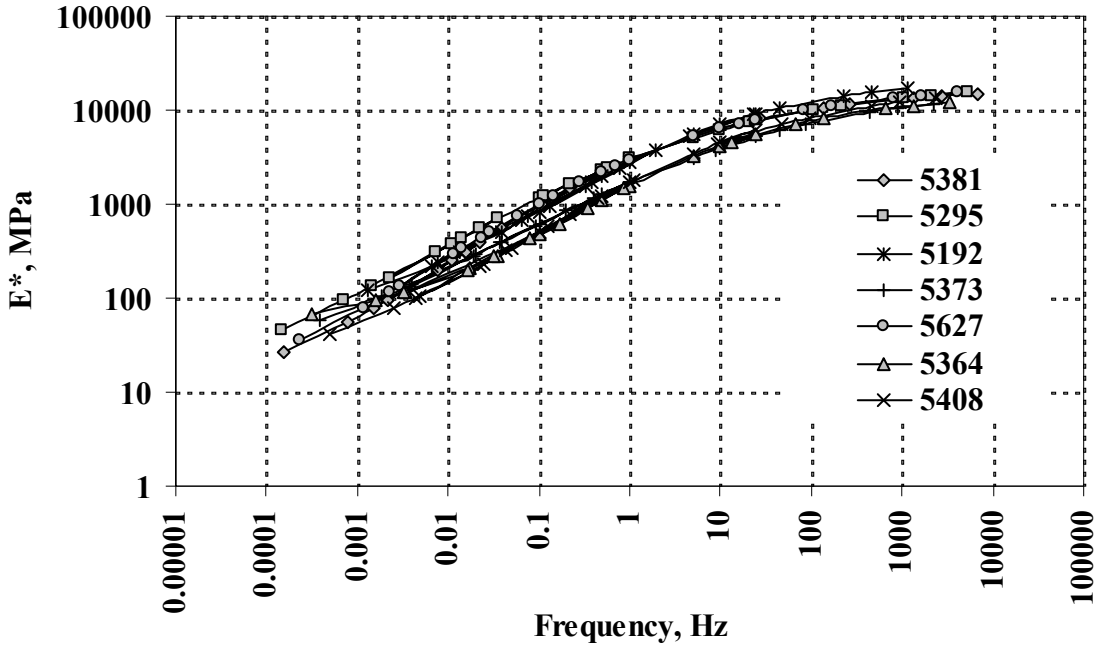

Fig. 1. JMF mix master curves

The measured dynamic modulus of all the specimens is tabulated in Table A2.2 (a) through (g). Fig.1 shows the master curves of the seven JMF mixes. The figure shows that there is variation among the seven mixes. The curves look similar in trend and the shifted frequencies vary between 0.0001 Hz and 100000 Hz. In terms of temperature, high frequency is analogous to low temperature and vice-versa. At low frequencies the curves exhibit a reasonable degree of separation, but at intermediate and high frequencies they tend to come closer to each other.

In order to verify if the dynamic moduli of the seven mixes are different and to determine the trend, the percent difference in the dynamic modulus of the mixes at each temperature and frequency were computed – summarized in Table A2.3 (a) through (d). The percent differences were then averaged over all the frequencies separately for each temperature. The trend and average percent difference between the mixes are summarized in Table 3. Projects 5627, 5295, and 5192 yielded the highest E* values, project 5364 yielded the lowest E* values among all projects. The difference between the mixes seems to increase as the testing temperature increases.

Table 3. Dynamic modulus trend and average difference of JMF mixes

	Trend												
4.4 (°C)	5364	<	5408	<	5381	<	5373	<	5627	<	5295	<	5192
avg. diff , %		9		5		7		8		3		6	
21.1 (°C)	5373	<	5364	<	5408	<	5381	<	5627	<	5295	<	5192
avg. diff, %		2		9		16		35		3		6	
37.8 (°C)	5364	<	5373	<	5408	<	5381	<	5627	<	5295	<	5192
avg. diff, %		23		9		31		6		4		8	
54.4 (°C)	5364	<	5408	<	5381	<	5373	<	5627	<	5295	<	5192
avg. diff, %		18		19		21		39		6		20	

To verify if the ± 2% change in aggregate gradation affected the dynamic modulus, the master curves of the JMF mixes and the modified mixes were compared as illustrated in Fig.A2.1 (a) through (g). Each JMF mix and the corresponding lower and upper modified mix are compared separately. The figure shows a small difference between the master curves at very low frequencies, which decreases as the frequency increases. This is similar to the trend observed among the JMF mixes. The modulus of a HMA layer/specimen at high temperatures (analogous to low frequencies) is a function of the interlocking between the aggregates since the asphalt in the mix tends to substantially lose its stiffness. Interlocking between the aggregates is affected by the gradation. Considering that the gradation of aggregates in the JMF mixes and the modified mixes are different, it is anticipated that the variation observed in the master curves at low frequencies is a manifestation of this HMA phenomenon. Conversely, as the temperature approaches very low values (frequency increases), the asphalt viscosity and stiffness increase substantially. Hence, the modulus is significantly influenced by the asphalt stiffness, which leads to the small difference between the mixes.

Statistical Analysis

A statistical analysis of variance (ANOVA) was performed to test if there is a significant difference among the JMF mixes, and between JMF and modified mixes. The data were analyzed using a multi-factor ANOVA using the statistical package SAS Version 9.1. Project, mix, temperature, and frequency were the treatment factors and dynamic modulus the response variable. The levels of the three treatment factors are summarized in Table 4.

Table 4. Levels of treatment factors

	Levels	
Block (Project)	7	5381, 5295, 5192, 5373, 5627, 5364, 5408
Mix	3	JMF, lower modified, upper modified
Temperature, ° C	4	4.4, 21.1, 37.8, 54.4
Frequency, Hz	6	25, 10, 5, 1, 0.5, 0.1

Initially, the block variable was tested to see if the seven blocks (projects) were different from each other. A Repeated Measures model was run with the forty-two specimens as the random subject variable. Repeated measure ANOVA was used because each specimen was tested under all dynamic modulus test conditions (four temperatures and six frequencies), and a standard ANOVA would fail to model the correlation between the repeated measures (test conditions). Also, in a standard ANOVA the data are assumed to be independent, which is invalid in this case. The model included Block, Mix, Temperature, Frequency and all two-factor interactions. Then the data were analyzed to see if there were any differences in the three levels of the mixes for the seven blocks. Here too, a repeated measures ANOVA (as above) was run using specimen as the random subjects, and all two factor interactions were included.

Table 5. Block pair-wise comparison p-values

Project	5381	5295	5192	5373	5637	5364	5408
5381	-	0.9295	0.4391	**0.0559**	0.9865	**0.0341**	0.1575
5295		-	0.9205	**0.0174**	0.9999	**0.0111**	**0.046**
5192			-	**0.0059**	0.7975	**0.0039**	**0.0141**
5373				-	**0.0245**	0.9991	0.9672
5627					-	**0.0154**	0.0665
5364						-	0.836
5408							-

To test the null hypothesis (i.e. there is no significant difference), a significance, or alpha level (α) of 0.05 was set before the analyses. The assumed α level was compared with the observed significance level (p-value) from the SAS output. If the p-value was smaller than α, null hypothesis was rejected. If the p-value was larger than the assumed alpha level null hypothesis was accepted.

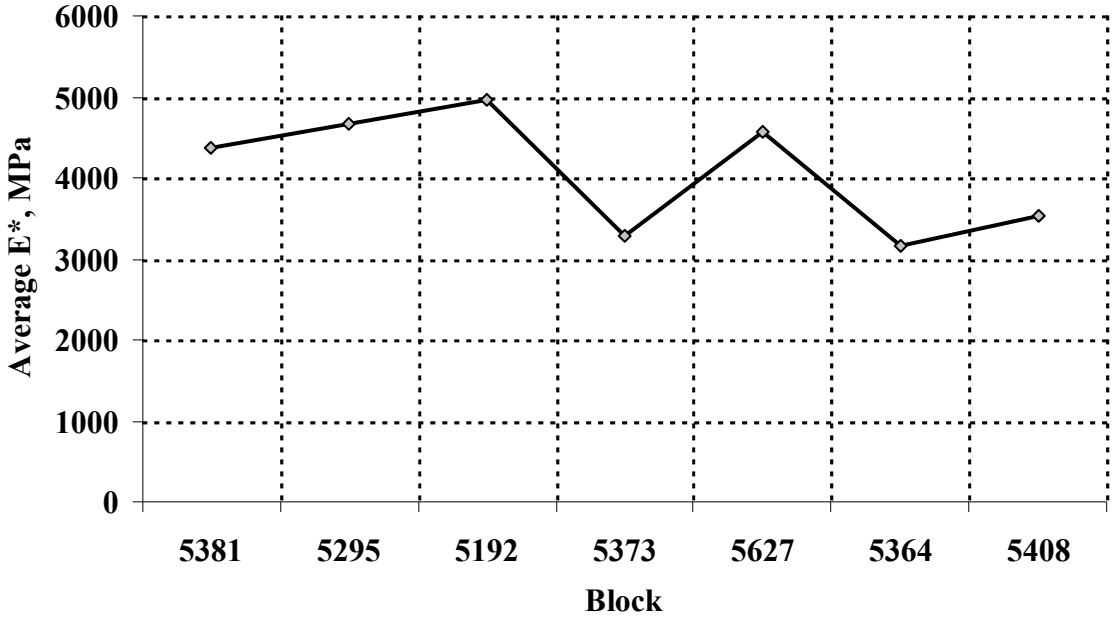

Fig. 2. Dynamic modulus trend

JMF Mixes

The p-values from the Tukey pair-wise comparisons of the seven blocks are summarized in Table 5. Project 5381 is significantly different from project 5364; marginally significant from project 5373; and insignificantly different from projects 5295, 5192, 5627, and 5408. Project 5373 is significantly different from projects 5627 and 5408; and insignificant from project 5364. Project 5364 is insignificantly different from project 5408. Generally speaking, the seven blocks (projects) are significantly different. This could also be verified by looking at the Type I p-value, which is an overall value indicating the presence of a significant difference among the factors analyzed. Type I p-value from SAS output was 0.0015 for the effect of the block (project), which indicates that the seven mixes are significantly different. Fig. 2 shows the mean dynamic modulus of the seven mixes used in the pair-wise comparisons. It shows the seven projects can be ranked as follows in terms of the average JMF E* values: 5364 < 5373<5408 < 5381 < 5627 < 5295 < 5192.

JMF versus Modified Mixes

To test if there is significant difference in the dynamic modulus between the JMF and modified mixes, and between the lower and upper modified mixes, the p-values from pair-wise comparisons within each block were analyzed. Table 6 shows the p-values from the Tukey pair-wise comparisons as well as Type I analysis. In all seven blocks, the p-values from the pair-wise comparisons of the lower and upper modified mixes, and JMF and modified mixes are mostly larger than 0.05. This indicates that there is generally no significant difference between the lower and upper modified mixes, and between the JMF and modified mixes. This could also be verified

by looking at the Type I p-values of all the seven blocks, which are larger than 0.05 (except for projects 5381 and 5364).

Table 6. JMF versus modified mix pair-wise comparison p-values

Project	Mix	UM	LM	Type I
5381	JMF	**0.0196**	0.0674	**0.0215**
	LM	0.2162	-	
5295	JMF	0.4824	0.6572	0.2259
	LM	0.2087	-	
5192	JMF	0.9999	0.8769	0.8514
	LM	0.872	-	
5373	JMF	0.1732	0.5857	0.1892
	LM	0.451	-	
5627	JMF	0.719	0.4825	0.5028
	LM	0.8817	-	
5364	JMF	0.4056	**0.0026**	**0.0016**
	LM	**0.0018**	-	
5408	JMF	0.8616	0.2081	0.2088
	LM	0.3342	-	

From the above discussions, it is clear that the dynamic modulus of the JMF mixes is significantly different. However, the difference is not generally significant between the JMF and the modified mixes (lower and upper modified mixes). In other words, dynamic modulus is not sensitive to the 2% variation in the percent passing sieve #200 aggregates in most of the mixes investigated.

MEPDG ANALYSIS

The MEPDG insists on calibrating/validating the mechanistic-empirical models incorporated in the guide to local conditions. Otherwise, the mechanistic computed fatigue damage cannot be used for predicting distress with any degree of confidence. The distress mechanisms are too complex to develop a practical model. Therefore, empirical factors and subsequent calibration is necessary to obtain realistic performance predictions. For fatigue cracking, none of the direct pavement responses like deflection, stress, or strain can be used to predict the rate of crack development. The Design Guide uses a complex algorithm to model the cracking mechanism that produces damage. As a result, the predicted damage must be correlated with actual cracking in the field. In the development of the flexible design procedure, rutting, fatigue cracking, and thermal cracking models have been calibrated using the design inputs and performance data largely from the LTPP database. Even though the LTPP database included sections located throughout many parts of North America, this national calibration may not be entirely adequate for specific regions of the country. The guide senses a need for more local or regional calibration.

The objectives of the MEPDG analysis were to (1) perform a simple evaluation of the distress prediction accuracy of the Design Guide (2) compare the predicted performance among JMF mixes and between JMF and modified mixes. However, calibrating the MEPDG prediction models is clearly not in the scope of this study. Version 1.000 of the MEPDG software was used in the analyses. The entire analysis was formed into two groups. In the first group, hereafter referred to as 'Level 1 Analysis', E*, G* and δ were the input parameters for the surface HMA layer. In the second group, hereafter referred to as the 'Level 3 Analysis', aggregate gradation and asphalt PG grade were input parameters for the surface HMA layer. All other inputs were a combination of Level 1 (site-specific data) and Level 3 (default values in the software).

Version 1.000 gives the user the option to choose either the NCHRP 1-37A viscosity based model or the NCHRP 1-40D G* based model as the HMA E* predictive model in the analyses. Since the G* based model is yet to be nationally calibrated, the viscosity based model was used in the analyses. Considering the fact that the JMF mixes were used in the construction of overlays, AC over AC rehabilitation type of analyses was performed. Site-specific traffic data was used only for the input parameters summarized in Table A3.1. For all other traffic inputs, default values in the software were used. Climatic files incorporated in the Design Guide were used for the EICM model. Either climatic files of the nearest weather station or a combination of weather stations closer to the location of the pavement section were used. In all cases, the water table was assumed to be 15m below the ground, which is close to field conditions. The different layers, type of material, and thickness are summarized in Table A3.2. In projects 5295, 5192, and 5364 a PCC layer was substituted with cement stabilized base layer to simplify the analysis because of lack of inputs. In all cases, default material properties in the software were used for the granular base, cement stabilized base, and subgrade layers. All unbound layers were assumed to be compacted. The material properties for the existing AC layer are summarized in Table A3.3. In all cases, a design life of 20 years was assumed.

Table 7. Field distress (averaged)

Project	5381	5295	5192	5373	5627	5364	5408
Survey date	Sep 2006	Oct 2006	Oct 2006	Sep 2006	Sep 2006	Aug 2006	Oct 2006
IRI (in/mi)	48.4	102.3	86.0	56.5	63.1	71.8	63.3
AC rutting (in)	0.15	0.04	0.073	0.16	0.06	0.33	0.14
Alligator cracking (%)	0	10.4	30.5	0.04	50.5	0	0.23
Longitudinal cracking (ft/mi)	0.62	54.5	16.4	11.3	0.92	0.79	1.7

The predictions for AC rutting, longitudinal cracking, alligator cracking, and IRI are summarized in Table A3.4 (Level 1) and A3.5 (Level 3). The output summary file generated by the Design Guide provides distress data for each month over the entire design life starting from the date of opening the pavement to traffic. However, only the distress data corresponding to the field distress survey date were used in the analyses. The field distress data for the seven projects are summarized in Table 7.

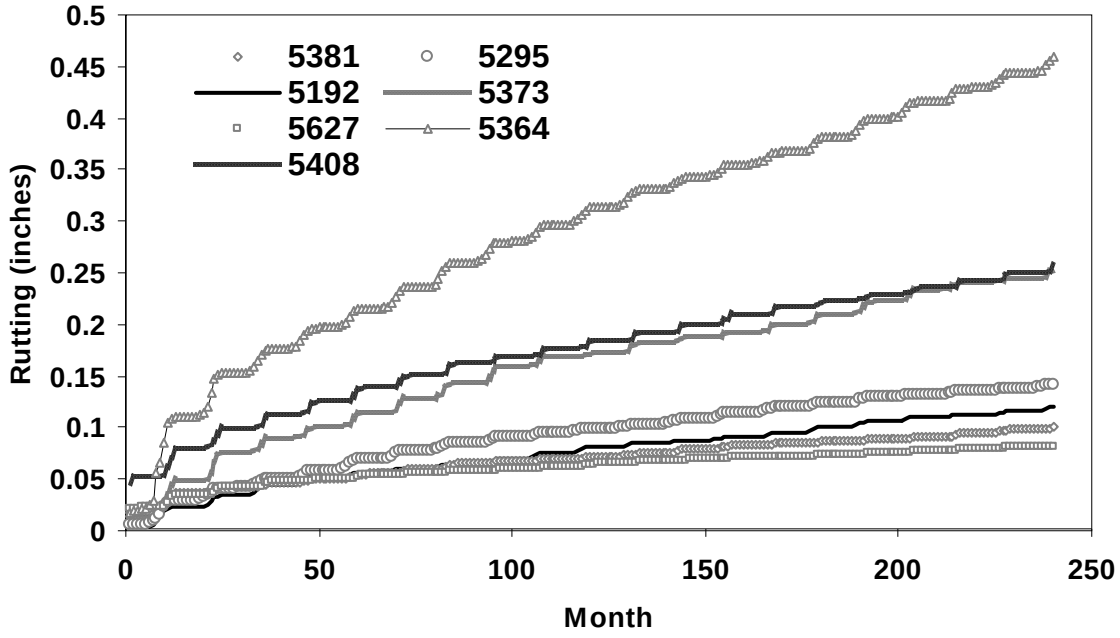

(a) Level 1

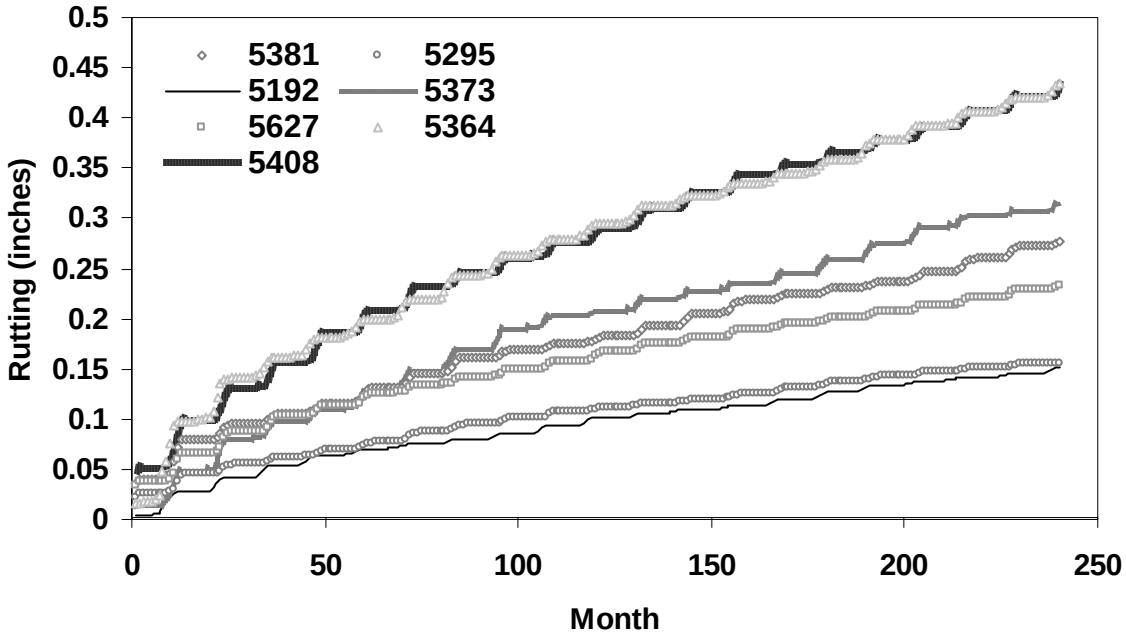

(b) Level 3

Fig. 3. Predicted AC rutting over the design life

Rutting

Rutting is a plastic/viscoplastic deformation in the form of surface depression in the wheel path in any or the entire pavement layers including the subgrade. It is caused mainly by heavy loads associated with high temperatures and/or poor mix. The predicted rut depths of the seven JMF

mixes over the design life are illustrated in Fig.3 (a) and (b). There is a significant variation among the mixes in both Level 1 and Level 3 predictions. Table 8 summarizes the average percent difference between the mixes at the end of the design life. It can be seen that the difference is larger in Level 1 predictions than Level 3 predictions. The Level 1 predicted rut depths of the seven projects as per the following sequence: 5627 < 5381 < 5192 < 5295 < 5373 < 5408 < 5364, whereas the Level 3 predicted rut depths as per the following sequence: 5192 < 5295 < 5373 < 5627 < 5408 < 5364. The trend followed by Level 3 predictions agree with the dynamic modulus trend of the JMF mixes, i.e., the rut depth is higher for mixes with lower dynamic modulus. This is in consistence with the results of the study conducted by Mohammad et al. (2006). They found that the predicted rut depths followed the same trend found in the dynamic modulus test results, particularly at high temperatures.

Table 8. Average percent rut depth difference (a) Level 1

Project	5381	5295	5192	5373	5627	5364	5408
5381	0	-42	-20	-152	18	-359	-155
5295		0	16	-77	42	-223	-80
5192			0	-110	31	-284	-113
5373				0	67	-82	-1
5627					0	-459	-211
5364						0	44
5408							0

(b) Level 3

	5381	5295	5192	5373	5627	5364	5408
5381	0	44	45	-14	16	-57	-56
5295		0	3	-102	-49	-178	-177
5192			0	-109	-54	-187	-186
5373				0	26	-38	-37
5627					0	-87	-86
5364						0	0.35
5408							0

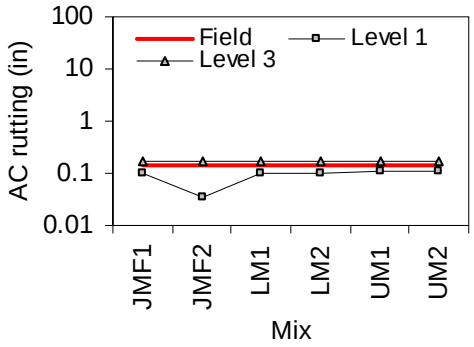

(a) 5381

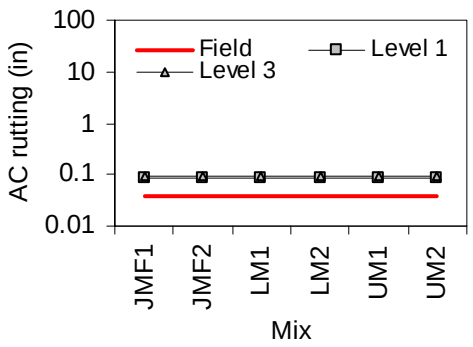

(b) 5295

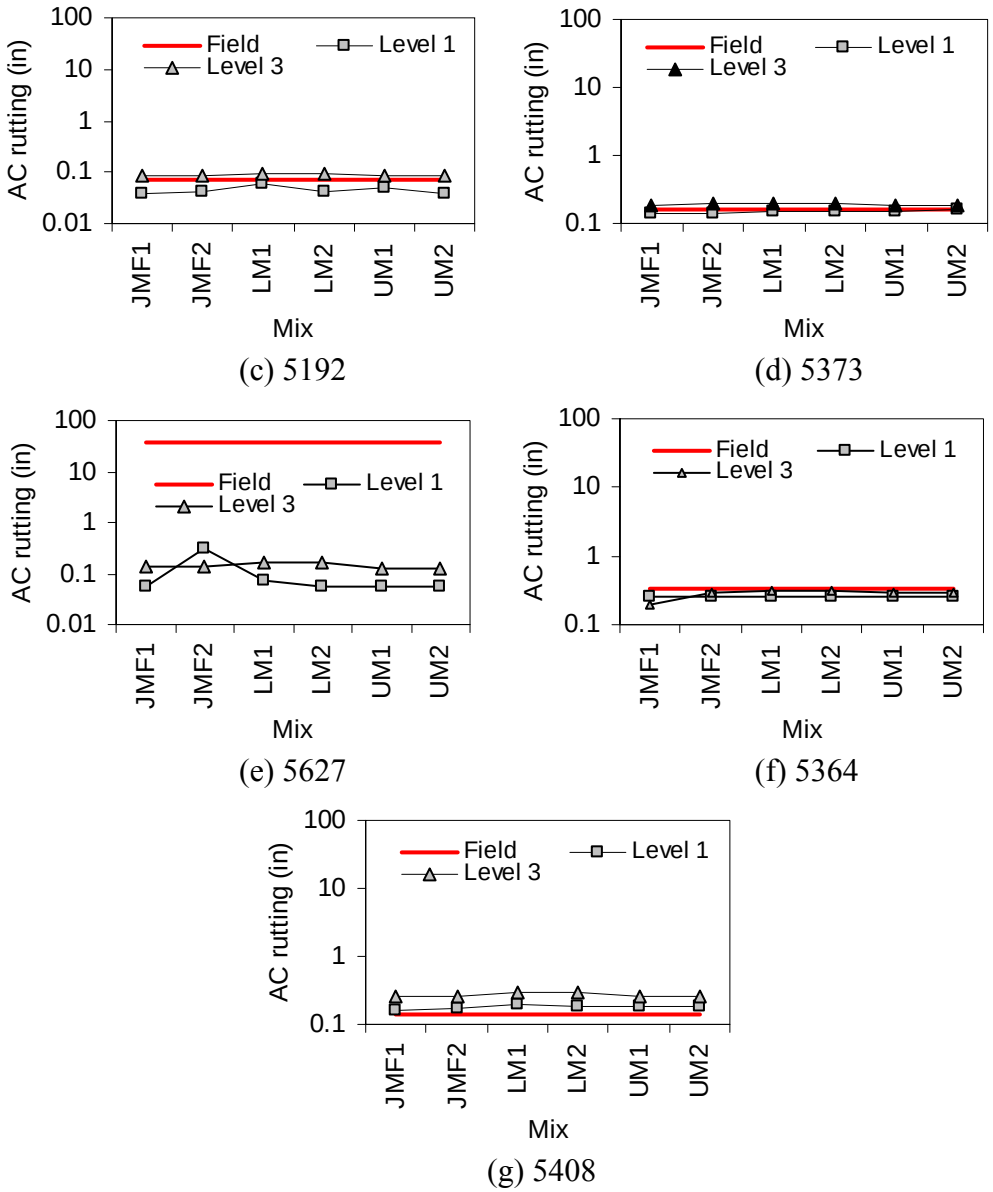

Fig. 4. Predicted and measured HMA rutting

Fig.4. (a) through (g) shows the Level 1 and Level 3 predicted HMA rutting. Level 3 predicted rut depths higher than the Level 1 predictions by an average of 46%. On average, Level 1 rut depths were lower than the field rut depth by 46% among the JMF mixes; 38% among LM and UM mixes. Level 3 rut depths were higher than the field rut depths by an average of 66% among JMF mixes; 75% among LM mixes and 63% among UM mixes. It appears from above that the rut depth of the three mixes show only a marginal variation. The ±2% change in the aggregate gradation in the modified mixes did not significantly affect the predicted rut depth. According to Hand et al. (2004), in all the cases they studied, predicted rut depths were higher than the measured rut depths by an average of about 90%. They also reported that Level 1 rutting performance models worked well. This agrees with the observations above wherein the Level 1

analysis under-predicted rut depths by about 40% while the Level 3 analysis over-predicted by about 60%. It is noteworthy that the rut depths for all the projects were relatively small.

Longitudinal Cracking

Longitudinal cracking is a type of fatigue failure associated with high tire pressures, wheel induced stresses, and severe aging of HMA layer near the surface. The predicted longitudinal cracking is shown in Fig. 5 (a) through (g). Longitudinal cracking predicted by Level 3 analysis were higher than those predicted by Level 1 by an average of 4 times even though they follow the same trend. In all cases the predicted cracking are significantly different form the field cracking. Except for projects 5295 and 5192, longitudinal cracking is over-predicted by the 2002 MEPDG. Level 1 prediction is higher than field cracking by an average of 11 times among JMF mixes; 17 times among LM mixes; and 11 times among UM mixes. The Level 3 predictions are higher by an average of 34 times among JMF mixes, 69 times among LM mixes; and 22 times among UM mixes. Similar to rutting, the predicted cracking does not differ between the three mixes in both Level 1 and Level 3 even though there is some inconsistency in Level 3. Clearly, the Design Guide over-predicted longitudinal cracking for the cases studied. Comparatively, Level 1 has predicted longitudinal cracking better than Level 3. Kim et al. (2006) studied the impact of 20 input parameters on the MEPDG flexible pavement performance models. They found that longitudinal cracking was sensitive to HMA layer thickness, nominal maximum aggregate size, and HMA volumetrics; and very sensitive to asphalt binder PG grade.

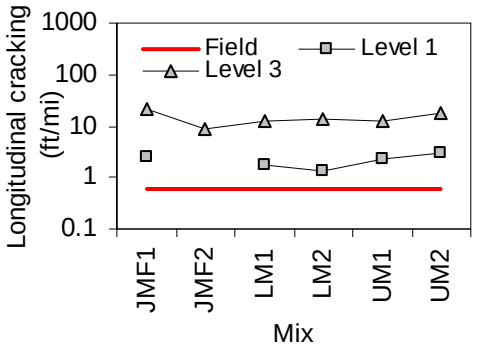

(a) 5381

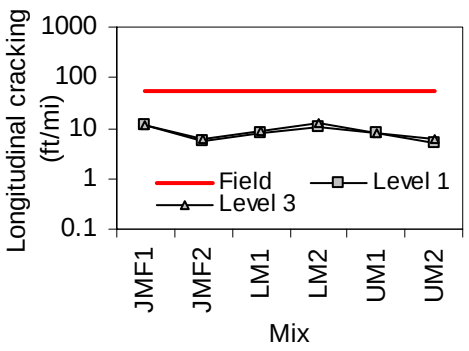

(b) 5295

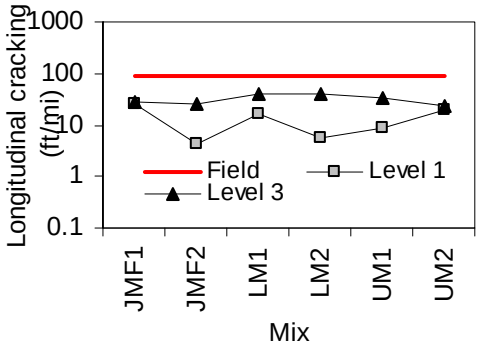

(c) 5192

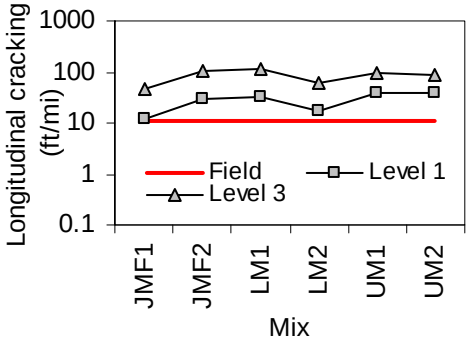

(d) 5373

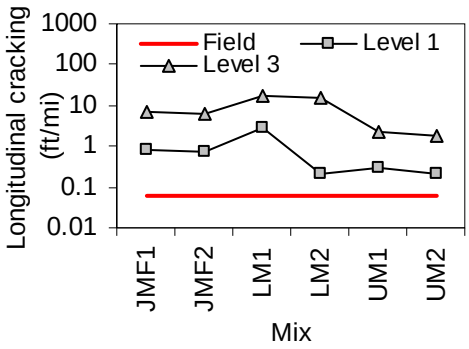

(e) 5627

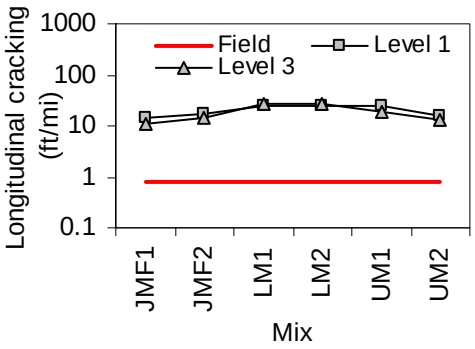

(f) 5364

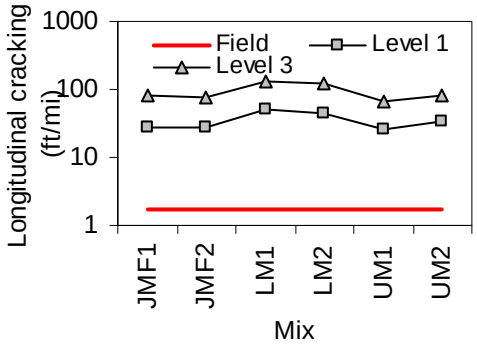

(g) 5408

Fig. 5. Predicted and measured longitudinal cracking

Alligator Cracking

Alligator cracking is a type of fatigue cracking which originates as short longitudinal cracks along the wheel path quickly spreading to form a chicken mesh/alligator pattern. These cracks propagate to the surface from the bottom of the HMA layer under repeated load applications. Alligator cracking is associated with heavy traffic volumes combined with high wheel loads and tire pressures resulting in high tensile strains at the bottom of the layer. Fig. 6 (a) through (g) illustrates the predicted alligator cracking compared with the field cracking. In all seven projects, the Level 1 and Level 3 predicted cracking to be close to zero. The predicted cracking agrees reasonably well with the field cracking, except for projects 5295, 5192, and 5627, which experienced different levels of cracking. The Design Guide has predicted alligator cracking reasonably well at both Level 1 and Level 3 for the cases studied (except for projects 5295, 5192, and 5627). In a comparative study Yang et al. (2004) used three pavement sections to compare measured and predicted alligator cracking. After 500,000 passes the measured alligator cracking was less than predicted cracking. However, they concluded that the difference was not significant considering the extremely low magnitudes of cracking encountered. Considering that the predicted cracking is almost negligible, it seems that alligator cracking may not be a critical distress in flexible pavement design. Kim et al. (2006) concluded that alligator cracking does not seem to be a critical distress in flexible pavement structures with relatively thick HMA layers. However, this cannot be generalized for all cases.

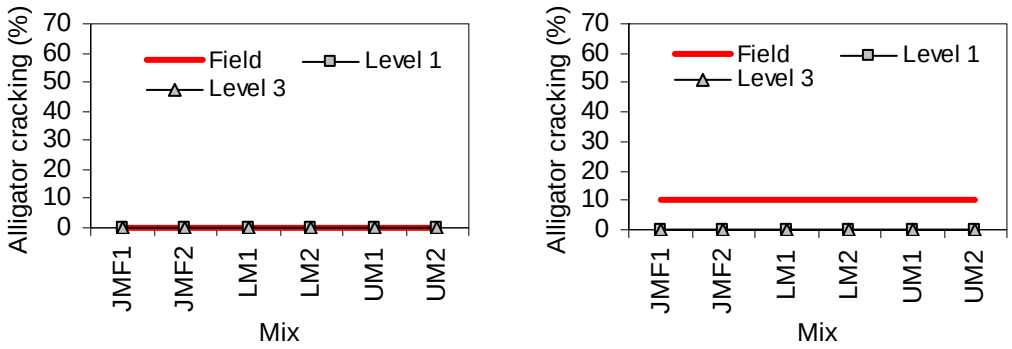

(a) 5381

(b) 5295

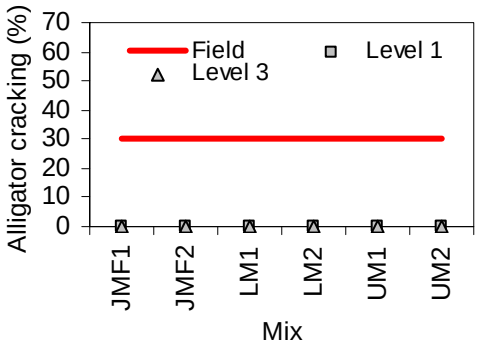

(c) 5192

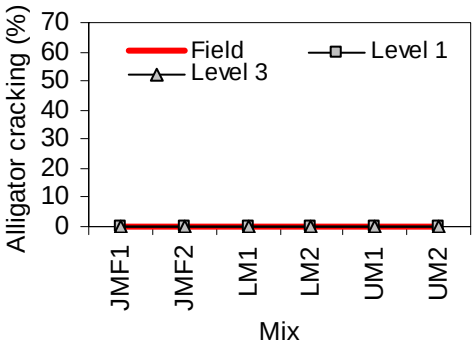

(d) 5373

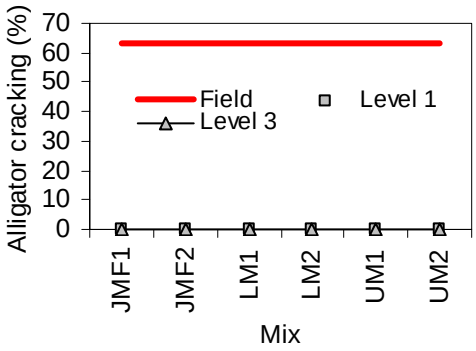

(e) 5627

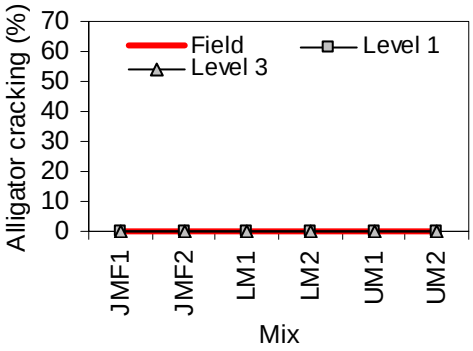

(f) 5364

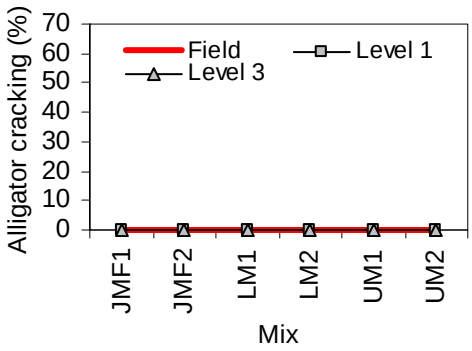

(g) 5408

Fig. 6. Predicted and measured alligator cracking

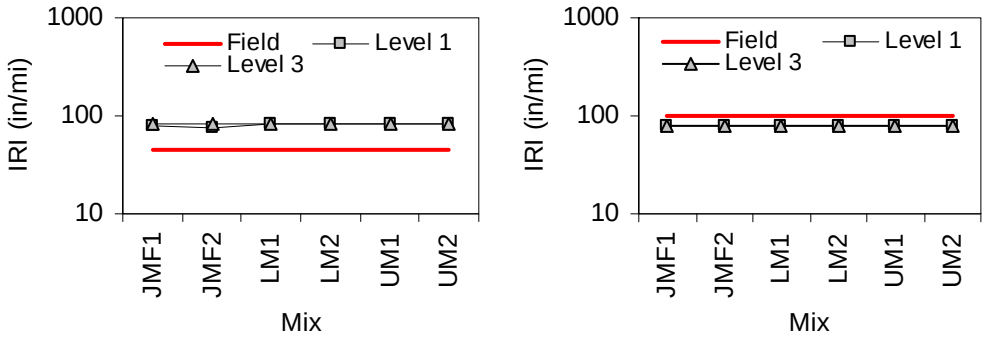

(a) 5381

(b) 5295

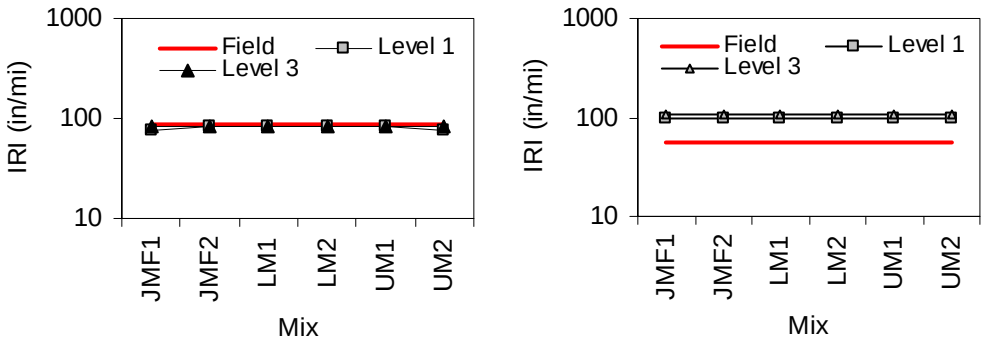

(c) 5192

(d) 5373

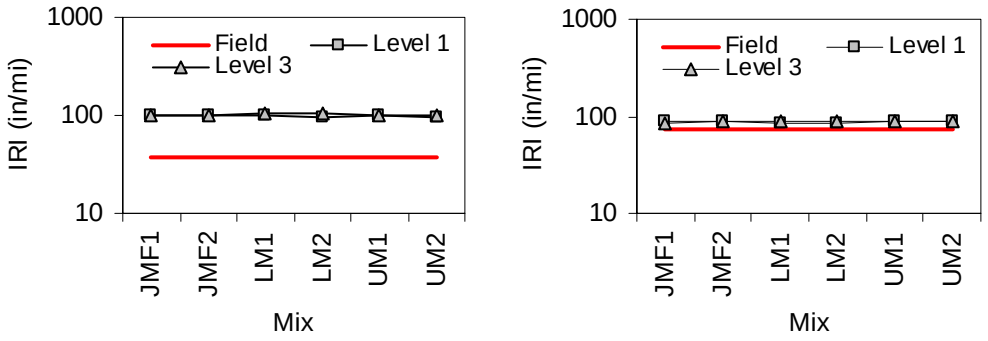

(e) 5627

(f) 5364

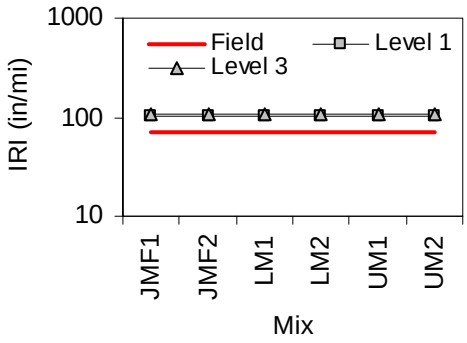

(g) 5408

Fig. 7. Predicted and measured IRI

International Roughness Index (IRI)

The Design Guide estimates IRI incrementally over the entire design period. The IRI model uses the predicted rutting, bottom-up/top-down fatigue cracking, thermal cracking, initial IRI, site factors, subgrade, and climatic factors to predict smoothness over time. IRI over the design life is a function of the as-constructed pavement profile. Fig. 7 (a) through (g) illustrates the predicted IRI and compared with the field IRI. Except for projects 5295 and 5192, in all other cases the Design Guide over-predicted IRI. Level 1 over predicted IRI by an average of 75% among JMF mixes; 76% LM mixes; and 77% among UM mixes. Level 3 predicted IRI were higher by an average of 83% among JMF mixes; 85% among LM mixes; and 83% among UM mixes. The predicted IRI do not show significant difference between the three mixes. Kim et al. (2006) also reported that IRI was not sensitive to most input parameters in their study. They stated that this may be due to the nature of the IRI model in the MEPDG which is a function of initial IRI, IRI due to distress, frost heave, and subgrade swelling.

Conclusions

1. The dynamic modulus of the seven JMF mixes selected for the study show reasonable variation. The difference is less significant at high frequencies but as the frequency decreases the difference becomes more prominent. In terms of temperature, the dynamic modulus varies significantly at high temperatures and marginally at low temperatures.
2. The dynamic modulus was insignificantly different between JMF and the modified mixes (lower and upper modified mixes), i.e., the ± 2% variation in percent passing sieve #200 did not produce a significant difference in dynamic modulus.
3. A statistical analysis of variance (ANOVA) confirmed that the seven JMF mixes were significantly different. It was also found that the JMF and modified mixes were not significantly different.
4. In all the projects, measured and predicted rut depths were relatively small. Level 1 predicted rutting was lower than field rutting by an average of 40%. Level 3 rut depths were higher by an average of 60%. The trend followed by predicted rut depths of the JMF mixes agreed reasonably well with the dynamic modulus trend; higher rut depths for the mixes with lower dynamic modulus. The difference in rutting between the JMF and modified mixes was insignificant.
5. The Design Guide over-predicted longitudinal cracking. Level 1 predicted about 13 times higher; Level 3 predicted about 28 times higher. However, the difference between the JMF and modified mixes was insignificant.
6. The Design Guide predicted alligator cracking reasonably well. In most cases, both Level 1 and Level 3 predicted cracking were close to zero. This agreed reasonably well with the field cracking for most of the projects. For the cases studied, alligator cracking appears not to be critical in terms of pavement performance.
7. IRI predicted by Level 1 and Level 3 analysis match reasonably well. However, the predicted IRI is higher than the field IRI by an average of 80%, which is a substantial difference. For the cases studied, predicted IRI was not sensitive to the mixes.
8. For the cases studied, the Level 3 predicted distresses higher than the Level 1 distresses. This could be attributed to the lack of confidence in the input data for Level 3, hence being

conservative, which lead to over-prediction. The difference was significant for rutting and longitudinal cracking, but insignificant for the IRI.

9. It is recommended to use Level 1 parameters for the prediction of rutting and longitudinal cracking. The results from this study showed that IRI and alligator cracking were not significantly affected by the choice of input level.
10. Except for alligator cracking, in all other cases the 2002 MEPDG was not successful in accurately predicting the distresses. In most cases, the predictions were higher than the field data. This could largely be due to the use of default values in the software as opposed to site-specific data in the analyses. This emphasizes the need to use site-specific data in the design/analysis in order to accurately and reliably predict distress data.
11. Generally, the ± 2% variation in aggregate gradation (passing #200) did not significantly affect the predicted distresses.

References

Ali, O. (2005). "Evaluation of the Mechanistic Empirical Pavement Design Guide (NCHRP 1-37A)." National Research Council Canada. Research Report 216.

Carvalho, R. L. (2006). "Mechanistic-Empirical Design of Flexible Pavements: A Sensitivity Study" M. S. Thesis, University of Maryland.

Ceylan, H., Gopalakrishnan, K., and Coree, B. (2005). "A Strategic Plan for Implementing the Mechanistic-Empirical Pavement Design Guide in Iowa." Presented at the 84th Annual Meeting of the Transportation Research Board, Washington, D.C., 2005.

Hall, K. D., and Beam, S., (2005). "Estimating the Sensitivity of Design Input Variables for Rigid Pavement Analysis with a Mechanistic-Empirical Design Guide." *Transportation Research Record*, 1919, 65 – 73.

Hand, A.J., Martin, A.E., Sebaaly, P.E., Weitzel, D., (2004). "Evaluating Field Performance: Case Study Involving Hot Mix Asphalt Performance-Related Specifications." *Journal of Transportation Engineering*, 130(2), 251-260.

Kim, S., Ceylan, H., Gopalakrishnan, K., and Heitzman, M., (2006). "Sensitivity Study of Iowa Flexible Pavements Using the Mechanistic-Empirical Pavement Design Guide." Presented at the 85th Annual Meeting of the Transportation Research Board, Washington, D.C., 2006.

Mohammad, L. N., Wu, Z., Obulareddy, S., Cooper, S., and Abadie, C., (2006). "Permanent Deformation Analysis of Hot-Mix Asphalt Mixtures with Simple Performance Tests and 2002 Mechanistic-Empirical Pavement Design Software." *Transportation Research Record*, 1970, 133 – 142.

Nantung, T., Chehab, G., Newbolds, S., Galal, K., Li, S., and Kim, D. H., (2005). "Implementation Initiatives of the Mechanistic-Empirical Pavement Design Guides in Indiana." *Transportation Research Record*, 1919, 142 – 151.

Robinette, C., and Williams, R. C. (2006). "The Effects of the Testing History and Preparation Method on the Superpave Simple Performance Test." *Journal of the Association of Asphalt Paving Technologists*.

Shah, A., McDaniel, R., and Gallivan, V., (2005). "Evaluation of Mixtures using Dynamic Modulus Tester: Results and Practical Considerations." *Journal of the Association of Asphalt Paving Technologists*, 74E.

Tandon, V., Bai, X., and Nazarian, S. (2006). "Impact of Specimen Geometry on Dynamic Modulus Measurement Test Setup." *Journal of Materials in Civil Engineering*, Vol. 18, No. 4, 477-484.

Yang, J., Wang, W., Petros, K., Sun, L., Sherwood, J., and Kenis, W., (2005). "Test of NCHRP 1-37A Design Guide Software for New Flexible Pavements." Presented at the 84th Annual Meeting of the Transportation Research Board, Washington, D.C., 2005.

APPENDIX 1

Table A1.1. Project details

Project	Pavement section	Year	SR	Location/ County	Milepost begin/end	Tonnage (tons)
5381	Railroad Crossing to Canyon Road, WA	1998	512	Tacoma/ Pierce	4.38/5.59	5695
5295	Thomas St. to N 152nd St., WA	1998	99	Seattle/ King	34.85/35.46	30335
5192	MP 0.0 to King County Line, WA	1997	99	Tacoma/ Pierce	0.50/1.05	2250
5373	V Mall Blvd. To Yak Riv Br. & Wapato Cr. To Ahtanum Cr., WA	1998	82	Yakima/ Yakima	36.31/38.05	12796
5627	Vic. Lind Coulee Bridge to Vic. SR 90, WA	1999	17	Moses lake/ Grant	43.00/45.22	15553
5364	Vancouver City Limits to S.E. 164th Ave., WA	1998	14	Vancouver/ Clark	6.58/7.93	31633
5408	SR 182 to SR 395, WA	1998	240	Richland/ Benton	37.78/40.18	30805

Table A1.2. Aggregate source, type and properties

	Mix ID						
	5381	5295	5192	5373	5627	5364	5408
Source	B-333	B-335	B-335	E-141	GT-18	G-106	R-7
County	Pierce	King	Pierce	Yakima	Grant	Clark	Benton
Type	Vashon recessional outwash gravels	Vashon glacial gravels	Vashon glacial gravels	Alluvial gravels/ terrace deposits	Outwash flood gravels	Outwash flood gravels	Alluvial gravels
G_{sb} (coarse aggregate)	2.681	2.703	2.650	2.712	2.783	2.718	2.643
G_{sb} (fine aggregate)	2.646	2.625	2.626	2.609	2.760	2.598	2.705
G_{sb} (aggregate blend)	2.653	2.646	2.631	2.653	2.771	2.603	2.699
Flat and elongated particles (%)	0[c]	0[b]	0[b]	0[b] 3[c]	4.15[a]	n/a	n/a
Single fractured faces (%)	100[b] 100[e]	100[f]	100[f]	94[b] 98[c] 100[e]	100[a] 100[b] 99.5[c] 98[e]	91[b] 93[c] 96[d]	96[b] 95[c] 100[g]
Un-compacted voids in fine aggregate (%)	47.9	49	49	46.3	49	n/a	n/a
Plastic fines in graded aggregate (%)	75	70	70	69	81	71	76

[a] (3/4" sieve); [b] (1/2" sieve); [c] (3/8" sieve); [d] (1/4" sieve); [e] (#4 sieve); [f] (#8 sieve); [g](#10 sieve)
n/a – not available

Table A1.3. WSDOT field tolerance limits for gradation and asphalt content

Sieve (mm)	Tolerance limits
19	± 6%
12.5	± 6%
9.5	± 6%
4.75	± 5%
2.36	± 4%
1.18	-
0.6	-
0.3	-
0.15	-
0.075	± 2%
AC	± 0.5%

Table A1.4. Quantitative variation of gradation after modification

Size (mm)	Mix ID													
	5381		5295		5192		5373		5627		5364		5408	
	L	U	L	U	L	U	L	U	L	U	L	U	L	U
25	-	-	-	-	-	-	2.0	-2.0	-	-	-	-	-	-
19	-	-	-	-	-	-	2.0	-2.0	-2.0	-2.0	-	-	-	-
12.5	2.0	-2.0	2.0	-2.0	-		2.0	-2.0	-2.0	-2.0	-2.0	-2.0	2.0	-2.0
9.5	2.0	-2.0	2.0	-2.0	-		2.0	-2.0	-2.0	-2.0	-2.0	-2.0	2.0	-2.0
4.75	2.0	-2.0	2.0	-2.0	2.0	-2.0	2.0	-2.0	-2.0	-2.0	-2.0	-2.0	2.0	-2.0
2.36	2.0	-2.0	2.0	-2.0	2.0	-2.0	2.0	-2.0	-2.0	-2.0	-2.0	-2.0	2.0	-2.0
1.18	2.0	-2.0	2.0	-2.0	2.0	-2.0	2.0	-2.0	-2.0	-2.0	-2.0	-2.0	2.0	-2.0
0.6	2.0	-2.0	2.0	-2.0	2.0	-2.0	2.0	-2.0	-2.0	-2.0	-2.0	-2.0	2.0	-2.0
0.3	2.0	-2.0	2.0	-2.0	2.0	-2.0	2.0	-2.0	-2.0	-2.0	-2.0	-2.0	2.0	-2.0
0.15	2.0	-2.0	2.0	-2.0	2.0	-2.0	2.0	-2.0	-2.0	-2.0	-2.0	-2.0	2.0	-2.0
0.075	2.0	-2.0	2.0	-2.0	2.0	-2.0	2.0	-2.0	-2.0	-2.0	-2.0	-2.0	2.0	-2.0
< 75µ	-38.8	37.3	-40.5	38.9	-25.5	24.5	-38.0	36.5	-32.0	30.7	-38.8	37.3	-38.8	37.3

L – Lower modified mix; U – Upper modified mix

All values are in percentage

Table A1.5. Properties of HMA test specimens

Mix ID		JMF1	JMF2	LM1	LM2	UM1	UM2
5381	AV	7.9	6.6	7.0	7.1	7.2	7.8
	G_{mb}	2.296	2.324	2.316	2.315	2.313	2.298
	V_{beff}	12.7	12.9	12.9	12.8	12.8	12.8
	Unit wt.	143	145	145	145	144	143
5295	AV	8.1	7.1	7.5	8.2	7.6	7.2
	G_{mb}	2.282	2.31	2.299	2.282	2.297	2.306
	V_{beff}	11.7	11.8	11.7	11.7	11.7	11.8
	Unit wt.	142	144	7.5	142	143	144
5192	AV	7	6.8	7.3	7.3	7.2	6.8
	G_{mb}	2.31	2.314	2.301	2.301	2.305	2.315
	V_{beff}	11.6	11.6	11.5	11.5	11.5	11.6
	Unit wt.	144	144	144	144	144	145
5373	AV	6.1	7.3	7.2	6.3	7.2	7.1
	G_{mb}	2.393	2.363	2.364	2.389	2.328	2.37
	V_{beff}	12.7	12.5	12.5	12.6	12.5	12.5
	Unit wt.	149	148	148	149	148	148
5627	AV	7.5	7.4	8.6	5.7	6.2	6
	G_{mb}	2.421	2.423	2.39	2.466	2.455	2.459
	V_{beff}	10.5	10.5	10.4	10.7	10.7	10.7
	Unit wt.	151.1	151.3	149.2	154.0	153.3	153.3
5364	AV	6.4	6.4	7.1	7.1	6.8	6.3
	G_{mb}	2.343	2.343	3.324	2.325	2.333	2.343
	V_{beff}	12.2	12.2	12.2	12.2	12.2	12.2
	Unit wt.	146	146	145	145	146	146
5408	AV	7.4	7.3	7.9	7.8	7.2	7.5
	G_{mb}	2.335	2.339	2.324	2.326	2.342	2.334
	V_{beff}	12.0	12.0	12.0	12.0	12.1	12.0
	Unit wt.	146	146	145	145	146	146

JMF1, JMF2 – field mix replicates; LM1, LM2 – lower modified mix replicates
UM1, UM2 – upper modified mix replicates
AV in percentage; V_{beff} in percentage; Unit wt. in pcf

Table A1.6. Test conditions (temperature and frequency in the order of testing)

Temperature	Mixture E*						Binder G*
° F	25 Hz	10 Hz	5 Hz	1 Hz	0.5 Hz	0.1 Hz	at 1.59 Hz
40	X	X	X	X	X	X	X
55							X
70	X	X	X	X	X	X	X
85							X
100	X	X	X	X	X	X	X
115							X
130	X	X	X	X	X	X	X

APPENDIX 2

Table A2.1. Binder G* and δ

		Temperature (° F)							
Mix ID		14	40	55	70	85	100	115	130
5381	G*	-	43105	12524	3150.8	660.2	151.2	33.1	9.11
	δ	-	36.1	48.7	59.3	67.9	74.7	79.6	83.3
	η	$7.2x10^{10}$	$9.51x10^{7}$	$5.51x10^{6}$	$5.05x10^{5}$	$7.27x10^{4}$	$1.42x10^{4}$	$3.7x10^{3}$	$1.19x10^{3}$
	A				16.4394				
	VTS				-5.7574				
5295	G*	-	56547	17859	4885.3	1218.8	298.2	76.7	23.8
	δ	-	33.3	44	53.8	60.7	66.6	68.6	73.6
	η	$4.9x10^{10}$	$1.45x10^{8}$	$1.10x10^{7}$	$1.20x10^{6}$	$1.94x10^{5}$	$4.03x10^{4}$	$1.08x10^{4}$	$3.45x10^{3}$
	A				14.5301				
	VTS				-5.0462				
5192	G*	-	65321	22644	5052.8	1257.5	273.2	62.2	8.64
	δ	-	30.9	41.9	55.4	64.9	73.2	76.5	82.2
	H	$6.4x10^{11}$	$3.78x10^{8}$	$1.6x10^{7}$	$1.14x10^{6}$	$1.36x10^{5}$	$2.29x10^{4}$	$5.31x10^{3}$	1.56x103
	A				17.039				
	VTS				-5.9679				
5373	G*	-	18161	4905.4	1203.3	291.2	79.8	23.6	9.8
	δ	-	41.2	50.9	57.8	62.3	63.4	61.9	62
	H	$1.8x10^{9}$	$1.43x10^{7}$	$1.66x10^{6}$	$2.57x10^{5}$	$5.45x10^{4}$	$1.42x10^{4}$	$4.58x10^{3}$	$1.71x10^{3}$
	A				13.7993				
	VTS				-4.7966				
5627	G*	-	26387	7486.5	1839.8	422	110	29.3	8.74
	δ	-	41.8	52.2	61.4	67.5	73	76.4	80.2
	η	$9.1x10^{9}$	$2.94x10^{7}$	$2.4x10^{6}$	$2.87x10^{5}$	$5.03x10^{4}$	$1.14x10^{4}$	$3.32x10^{3}$	$1.16x10^{3}$
	A				15.3901				
	VTS				-5.3792				
5364	G*	-	29451	9229.9	2437.5	568.1	131.3	28.4	8.9
	δ	-	38.2	47.7	57.1	65.2	71.7	75.9	80.8
	H	$3.1x10^{10}$	$6.04x10^{7}$	$4.03x10^{6}$	$4.11x10^{5}$	$6.4x10^{4}$	$1.33x10^{4}$	$3.61x10^{3}$	$1.2x10^{3}$
	A				16.0001				
	VTS				-5.5986				
5408	G*	-	31156	9275.5	2360.3	546	131	28.6	8.72
	δ	-	38.3	48.1	57.5	65.7	72	76.7	81.5
	η	$3.2x10^{10}$	$6.01x10^{7}$	$3.98x10^{6}$	$4.03x10^{5}$	$6.26x10^{4}$	$1.3x10^{4}$	$3.52x10^{3}$	$1.17x10^{3}$
	A				16.0605				
	VTS				-5.6210				

G* in kPa; δ in degrees; η in cP

Table A2.2. Measured dynamic modulus (a) Mix ID 5381

Temp	Freq	Dynamic modulus, MPa					
		JMF1	JMF2	LM1	LM2	UM1	UM2
4.4	25	15794	16215	15059	15534	15459	15694
	10	14387	14859	13514	14015	13799	14097
	5	13311	13753	12646	12697	12600	12835
	1	10796	11089	10118	9919	9789	10087
	0.5	9778	10221	9042	8748	8468	8828
	0.1	7367	7331	6553	6253	5784	5866
21.1	25	7216	7884	6641	6943	6459	6704
	10	5856	6250	5393	5537	4973	5065
	5	4888	5082	4586	4633	3959	4000
	1	2985	2888	2754	2709	2179	2155
	0.5	2254	2141	2093	2093	1593	1592
	0.1	1106	972	1023	1027	690.1	697.4
37.8	25	2681	2638	1691	2635	1490	1939
	10	1907	1490	1192	1376	903.4	1182
	5	1389	1012	834.3	939.9	594.9	801
	1	577.2	390.8	321.7	379.6	220.3	361.3
	0.5	378.1	267.7	215.3	263.9	151	283.7
	0.1	143.3	118.8	89.4	116.4	74.7	190.1
54.4	25	282.3	692.3	609.9	1162	388.8	574.5
	10	339.1	287.5	292.6	694.4	222.6	302.6
	5	210.7	168.3	182.2	447.3	157.2	191.9
	1	65.1	62.6	63.8	153.9	78.3	82.7
	0.5	49.2	48.4	48.8	109	66.9	73.5
	0.1	26.9	30.2	30.5	61.3	52.3	53.7

Table A2.2. (b) Mix ID 5295

Temp	Freq	Dynamic modulus, MPa					
		JMF1	JMF2	LM1	LM2	UM1	UM2
4.4	25	15922	17732	14672	15534	17137	18463
	10	14553	16061	13300	14015	15633	16909
	5	13496	14804	12280	12697	14583	15694
	1	10839	11750	9633	9919	11831	13014
	0.5	9608	10371	8582	8748	10812	11876
	0.1	6870	7559	6259	6253	8010	8934
21.1	25	7688	8461	6930	6943	8357	9190
	10	6208	6837	5710	5537	6685	7613
	5	5330	5672	4832	4633	5702	6551
	1	3255	3468	3035	2709	3676	4210
	0.5	2564	2750	2399	2093	2943	3444
	0.1	1351	1473	1375	1027	1612	1932
37.8	25	2255	3431	2346	2635	2676	2761
	10	1496	2392	1660	1376	1922	1912
	5	1095	1805	1238	939.9	1482	1415
	1	482.2	860	647.6	379.6	710.8	658.2
	0.5	339.4	619.5	510.9	263.9	507.5	483.7
	0.1	161.1	284.4	323.8	116.4	240.8	242.3
54.4	25	759.8	776.7	931.6	1162	701.1	1322
	10	491.3	456.9	651.1	694.4	693.6	701.5
	5	331.6	305.6	513.1	447.3	394.2	482.6
	1	123.2	126.3	328.4	153.9	247.2	199.3
	0.5	91.1	98.4	286	109	182.5	144.6
	0.1	49.5	54.9	222.7	61.3	97.2	70.9

Table A2.2. (c) Mix ID 5192

Temp	Freq	Dynamic modulus, MPa					
		JMF1	JMF2	LM1	LM2	UM1	UM2
4.4	25	16649	17185	14458	16550	16458	18428
	10	15454	15718	13230	15519	15181	17001
	5	14561	14581	12283	14651	13932	15939
	1	12511	11703	10059	12310	11259	13389
	0.5	11581	10419	9234	11248	10136	12240
	0.1	9229	7610	7004	8908	7545	9585
21.1	25	8855	7729	6925	8799	7730	9250
	10	7452	6236	5602	7368	6303	7721
	5	6530	5113	4802	6403	5182	6739
	1	4425	3068	3101	4438	3174	4426
	0.5	3665	2473	2447	3701	2516	3536
	0.1	2172	1206	1365	2190	1296	2087
37.8	25	2654	2292	1747	2861	2218	1798
	10	1916	1521	1294	2100	1456	1885
	5	1438	1065	926.4	1649	1032	1423
	1	679.1	417.4	390.8	779.8	403.9	658.1
	0.5	481.5	276	273.2	554.1	268.4	450.9
	0.1	209.2	110.1	123.6	236	105.3	191.2
54.4	25	975.6	2558	847.3	2956	571.3	2037
	10	618	1677	583.4	906.5	332.5	844.2
	5	426.1	1145	407.7	638.6	208.6	575.2
	1	154.5	428	147.7	238.8	70.3	208.5
	0.5	107.4	281.1	104.5	156.2	53.7	140
	0.1	52.2	145.7	78.3	68.9	31	67.4

Table A2.2. (d) Mix ID 5373

Temp	Freq	Dynamic modulus, MPa					
		JMF1	JMF2	LM1	LM2	UM1	UM2
4.4	25	14193	11702	11996	13146	11428	11658
	10	12844	10648	10486	11550	9868	10067
	5	11433	9671	9251	10353	8729	8765
	1	8804	7260	6640	7687	6079	6002
	0.5	7778	6284	5717	6614	5126	5020
	0.1	5497	4242	3712	4505	3245	3097
21.1	25	5911	4863	4450	5279	3957	4082
	10	4636	3666	3246	4121	3001	3058
	5	3878	2923	2554	3272	2347	2389
	1	2333	1652	1343	1869	1243	1213
	0.5	1833	1288	1024	1456	938.2	910.1
	0.1	1015	716.6	522.3	808.7	455.8	464.3
37.8	25	1781	1630	888.2	1420	859.1	1042
	10	1344	933.1	703.1	983.9	652.5	663.1
	5	1005	677.7	503.4	724.7	478.4	474.8
	1	472.2	345.2	236.5	352.4	209.6	220.9
	0.5	354.9	276.6	188.3	277.9	159.6	179.3
	0.1	184.2	170.5	107.5	160.8	88.4	109.8
54.4	25	320	1549	1132	502.8	888.1	440.9
	10	416.6	330.2	344.4	353.7	23.5	285.1
	5	297.7	217.8	220.4	257.7	8.9	192.8
	1	123.5	112.4	93.5	138.2	72.5	96.8
	0.5	101.5	95.7	79.8	118.3	64.5	82.1
	0.1	66.2	64	52.3	82.6	31.1	59.9

Table A2.2. (e) Mix ID 5627

Temp	Freq	Dynamic modulus, MPa					
		JMF1	JMF2	LM1	LM2	UM1	UM2
4.4	25	17178	16522	15992	15036	15324	17668
	10	15315	15222	14371	13480	14070	15832
	5	14240	13827	13155	12362	13350	13901
	1	11347	10767	10263	9760	10943	10655
	0.5	9866	9382	9212	8782	9789	9391
	0.1	7103	6574	6539	6402	7106	6522
21.1	25	7707	7676	7555	7389	7879	7461
	10	6488	6139	6177	5893	6415	5916
	5	5523	4914	5055	4912	5135	4713
	1	3364	2732	3070	3021	3174	2780
	0.5	2731	2103	2560	2358	2554	2132
	0.1	1427	1009	1540	1251	1327	1023
37.8	25	3175	3044	3002	2341	2531	2593
	10	2442	1834	2323	1538	1491	1660
	5	1841	1293	1856	1133	1064	1194
	1	841.4	541.7	1346	507.6	453.5	490.9
	0.5	576.2	365	1153	362.2	318.1	333.5
	0.1	257.9	159.3	953.5	168.3	148.1	140.2
54.4	25	716.5	849.7	590.5	1732	788.7	1285
	10	631.3	414.7	390.6	586.5	574.9	486.5
	5	408.1	252.8	274.1	396.6	379.7	308.5
	1	144.3	90	120.2	146.2	134.9	115.9
	0.5	99.8	69.4	99.8	106.1	99.8	83.2
	0.1	52.6	41.4	74.3	55	55	48.5

Table A2.2. (f) Mix ID 5364

Temp	Freq	Dynamic modulus, MPa					
		JMF1	JMF2	LM1	LM2	UM1	UM2
4.4	25	14418	12964	14495	14663	13084	13895
	10	12247	11738	13070	13345	11587	12199
	5	10944	10696	11985	12319	10211	10889
	1	7815	7831	9548	9868	7405	7852
	0.5	6541	6756	8535	8790	6477	6571
	0.1	4202	4475	6227	6278	4410	4183
21.1	25	5040	5393	6298	6755	5178	5174
	10	3950	4286	5261	5442	3899	3800
	5	3088	3273	4385	4426	3004	3054
	1	1554	1729	2642	2747	1515	1601
	0.5	1121	1262	2073	2211	1105	1166
	0.1	526.5	579.1	1089	1154	582.7	581.5
37.8	25	1244	1332	2029	1899	1258	1139
	10	797.4	819.1	1315	1321	759.9	679.3
	5	572.6	560.4	935.9	972	508.3	449.3
	1	292.5	232.3	392.6	424.7	212.2	173.1
	0.5	239.3	171	273.4	299.8	158.8	128.1
	0.1	167.4	95.8	123.8	132.2	95.2	66.2
54.4	25	635.3	511.4	670.8	936.9	498.5	492.9
	10	425.7	306.3	400.1	426.3	317.3	306.6
	5	324.2	214.2	254.8	265.7	237.5	219.1
	1	213.6	114.2	93.6	98.7	151.2	123
	0.5	191.1	98.4	69.2	72.3	137.7	108.8
	0.1	157.5	77.8	40.3	39.8	117.2	88.6

Table A2.2. (g) Mix ID 5408

Temp	Freq	Dynamic modulus, MPa					
		JMF1	JMF2	LM1	LM2	UM1	UM2
4.4	25	14747	13904	12472	13676	14998	13988
	10	13186	12285	11050	11917	13193	12800
	5	12006	10915	9724	10613	11982	11522
	1	9140	8073	7039	7783	8876	8188
	0.5	7891	7022	6100	6520	7581	6944
	0.1	5317	4649	4088	4268	4806	4519
21.1	25	6378	5699	5189	5244	5967	5728
	10	4918	4436	4040	4159	4491	4304
	5	4025	3497	3242	3333	3497	3426
	1	2348	1904	1702	1763	1923	1756
	0.5	1793	1386	1252	1287	1449	1245
	0.1	907.8	659.5	564.1	596.2	663.1	541.1
37.8	25	2217	1490	1359	1544	1502	1459
	10	1425	929.8	834	982.3	950.5	885.6
	5	1022	636.4	563.8	678.9	664.5	593.5
	1	452	247.3	226.4	291.4	304.8	238
	0.5	324.1	172.8	158.3	212.9	234.5	172.4
	0.1	157.8	83.8	71.2	113.6	140.6	92.9
54.4	25	741.8	785.4	490.1	513.5	500.8	516.3
	10	376.4	434.8	271.3	281	280	327.5
	5	236.7	275.6	172.7	178.9	184.7	236.2
	1	95.9	100.2	60.8	64.6	68.6	133.4
	0.5	73.7	76.5	46.5	79.4	54.2	115.4
	0.1	45.1	47.6	28.6	51	35	88.7

Table A2.3. Percent difference in E* of JMF mixes (a) 4.4 °C

Freq (Hz)	Project	5381	5295	5192	5373	5627	5364	5408
25	5381	-	-15	-24	-9	-11	3	-8
	5295		-	-8	5	3	16	6
	5192			-	12	10	22	13
	5373				-	-2	11	2
	5627					-	13	3
	5364						-	-11
	5408							-
10	5381	-	-14	-23	-7	-11	4	-6
	5295		-	-8	6	3	15	7
	5192			-	13	10	22	14
	5373				-	-4	10	1
	5627					-	13	4
	5364						-	-10
	5408							-
5	5381	-	-13	-22	-5	-10	4	-5
	5295		-	-7	7	3	15	7
	5192			-	14	10	21	14
	5373				-	-5	9	0
	5627					-	13	5
	5364						-	-10
	5408							-
1	5381	-	-12	-18	1	-9	6	-2
	5295		-	-6	11	3	16	9
	5192			-	16	8	21	14
	5373				-	-9	5	-2
	5627					-	13	7
	5364						-	-8
	5408							-
0.5	5381	-	-11	-16	4	-8	7	1
	5295		-	-5	13	3	16	10
	5192			-	17	7	20	14
	5373				-	-12	4	-3
	5627					-	14	8
	5364						-	-7
	5408							-
0.1	5381	-	-8	-10	12	-5	12	7
	5295		-	-2	18	3	18	13
	5192			-	19	4	20	15
	5373				-	-19	0	-6
	5627					-	16	11
	5364						-	-6
	5408							-

Table A2.2. (b) 21.1 °C

Freq (Hz)	Project	5381	5295	5192	5373	5627	5364	5408
25	5381	-	-8	-17	11	-6	9	5
	5295		-	-8	17	2	16	12
	5192			-	23	9	22	19
	5373				-	-19	-1	-6
	5627					-	15	10
	5364						-	-5
	5408							-
10	5381	-	-7	-14	15	-5	13	9
	5295		-	-6	21	2	18	15
	5192			-	25	8	23	20
	5373				-	-24	-3	-8
	5627					-	17	13
	5364						-	-4
	5408							-
5	5381	-	-5	-11	19	-3	16	12
	5295		-	-5	23	2	21	17
	5192			-	27	7	24	21
	5373				-	-28	-3	-8
	5627					-	19	15
	5364						-	-5
	5408							-
1	5381	-	-2	-3	28	1	27	22
	5295		-	0	30	3	29	24
	5192			-	30	3	29	24
	5373				-	-39	-1	-9
	5627					-	27	21
	5364						-	-8
	5408							-
0.5	5381	-	-1	1	32	3	33	27
	5295		-	2	33	3	34	27
	5192			-	32	1	33	26
	5373				-	-44	1	-9
	5627					-	32	25
	5364						-	-10
	5408							-
0.1	5381	-	2	10	41	8	49	38
	5295		-	8	40	5	47	36
	5192			-	35	-2	43	31
	5373				-	-57	13	-5
	5627					-	45	33
	5364						-	-21
	5408							-

Table A2.2. (c) 37.8 °C

Freq (Hz)	Project	5381	5295	5192	5373	5627	5364	5408
25	5381	-	-5	-17	30	-5	29	20
	5295		-	-11	33	0	32	24
	5192			-	40	10	39	31
	5373				-	-49	-1	-14
	5627					-	32	24
	5364						-	-12
	5408							-
10	5381	-	-5	-14	33	-5	36	25
	5295		-	-8	36	1	40	28
	5192			-	41	8	44	34
	5373				-	-56	6	-12
	5627					-	39	28
	5364						-	-19
	5408							-
5	5381	-	-6	-12	35	-5	42	28
	5295		-	-6	38	1	46	32
	5192			-	42	7	49	36
	5373				-	-60	12	-10
	5627					-	45	31
	5364						-	-25
	5408							-
1	5381	-	-10	-10	36	-5	54	35
	5295		-	0	42	4	58	41
	5192			-	42	4	58	41
	5373				-	-65	27	-2
	5627					-	56	39
	5364						-	-39
	5408							-
0.5	5381	-	-13	-10	36	-6	57	38
	5295		-	2	43	6	61	45
	5192			-	41	3	61	43
	5373				-	-65	33	3
	5627					-	59	41
	5364						-	-44
	5408							-
0.1	5381	-	-22	-15	30	-9	58	41
	5295		-	6	42	10	65	51
	5192			-	38	5	63	48
	5373				-	-55	40	16
	5627					-	61	46
	5364						-	-41
	5408							-

Table A2.2. (d) 54.4 °C

Freq (Hz)	Project	5381	5295	5192	5373	5627	5364	5408
25	5381	-	-19	-51	24	-25	36	14
	5295		-	-26	37	-4	47	28
	5192			-	50	17	58	43
	5373				-	-65	16	-14
	5627					-	49	31
	5364						-	-35
	5408							-
10	5381	-	-26	-55	20	-30	38	14
	5295		-	-23	37	-3	51	32
	5192			-	49	16	60	45
	5373				-	-62	23	-7
	5627					-	52	34
	5364						-	-39
	5408							-
5	5381	-	-32	-59	15	-34	38	14
	5295		-	-21	36	-1	53	35
	5192			-	47	16	61	46
	5373				-	-58	26	-2
	5627					-	53	36
	5364						-	-38
	5408							-
1	5381	-	-49	-73	-3	-44	24	10
	5295		-	-16	31	3	49	39
	5192			-	41	17	56	48
	5373				-	-40	26	12
	5627					-	47	37
	5364						-	-20
	5408							-
0.5	5381	-	-57	-81	-14	-48	12	6
	5295		-	-16	27	6	44	40
	5192			-	37	18	51	48
	5373				-	-30	23	18
	5627					-	41	37
	5364						-	-6
	5408							-
0.1	5381	-	-74	-105	-47	-56	-43	-5
	5295		-	-18	16	11	18	40
	5192			-	28	24	31	49
	5373				-	-6	3	29
	5627					-	9	33
	5364						-	27
	5408							-

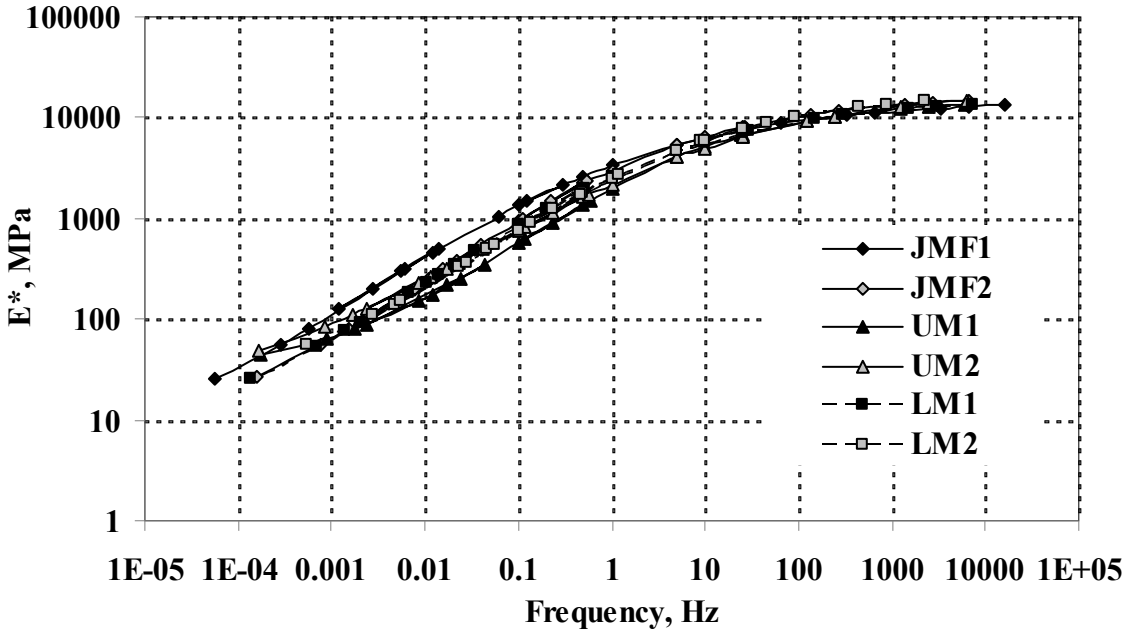

(a) Mix ID 5381

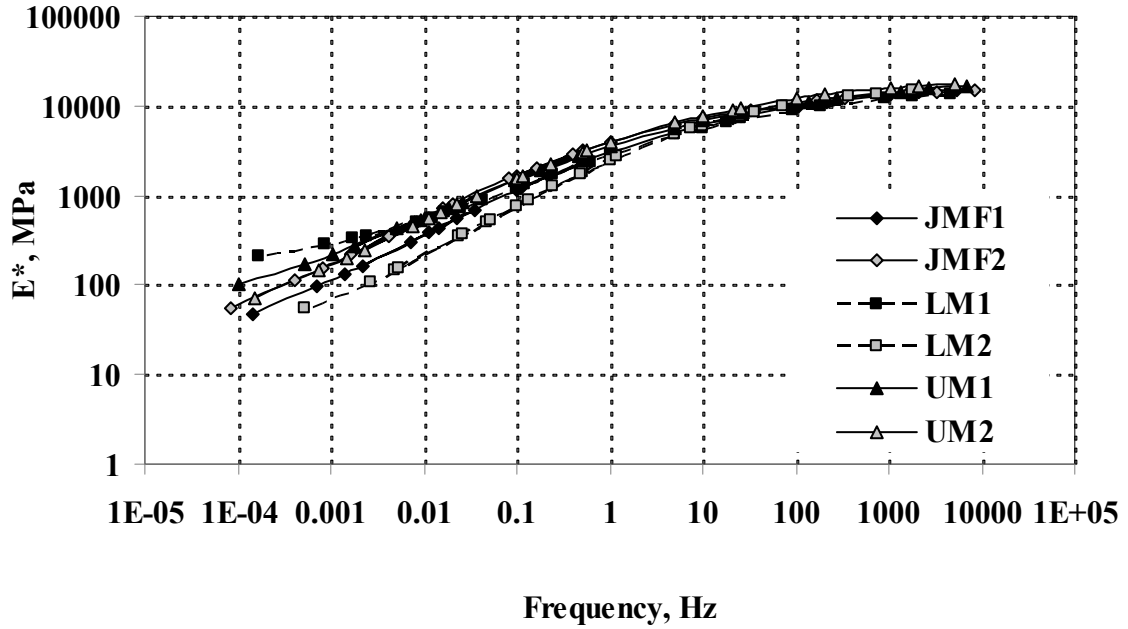

(b) Mix ID 5295

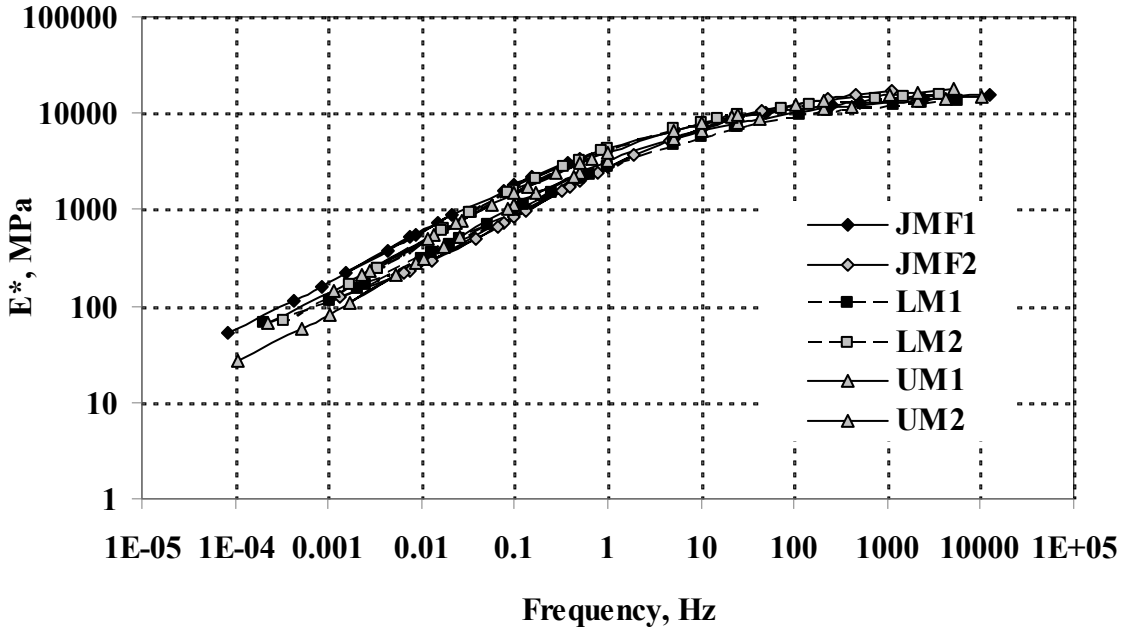

(c) Mix ID 5192

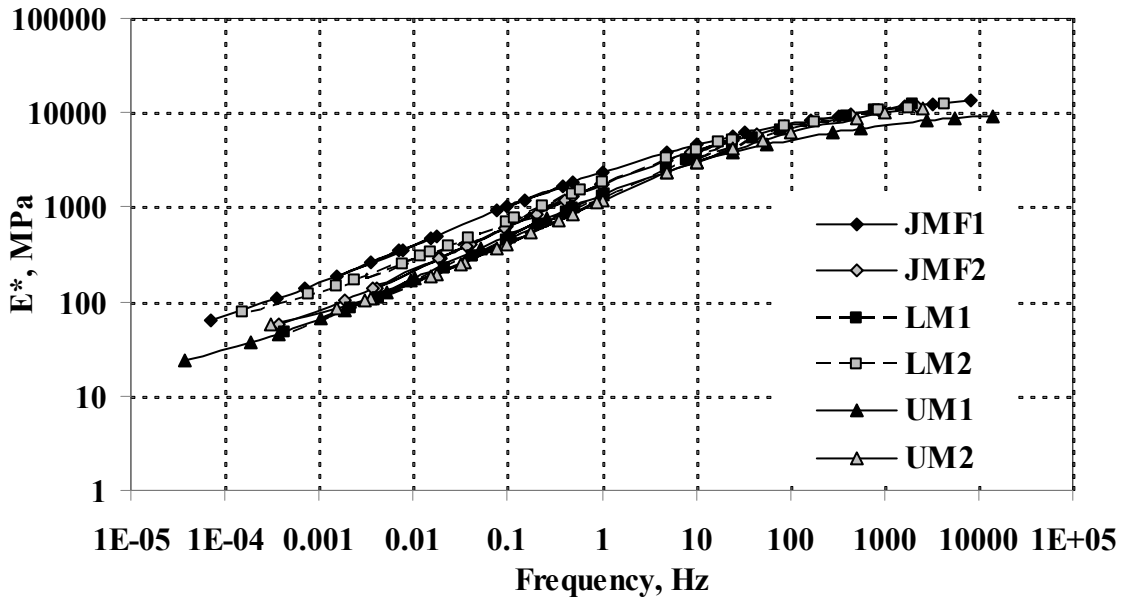

(c) Mix ID 5373

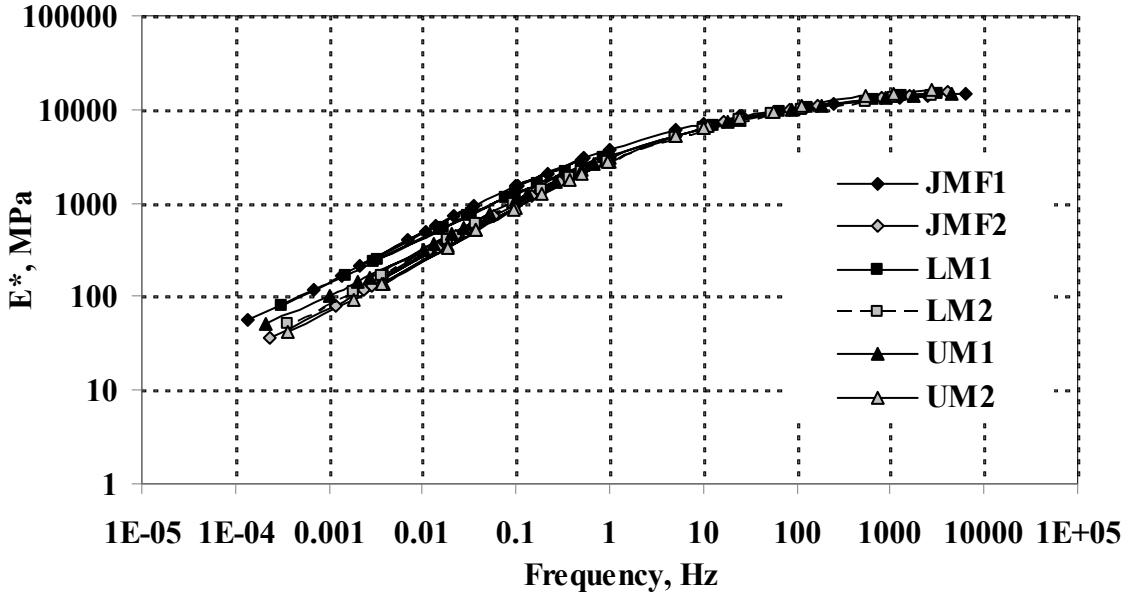

(e) Mix ID 5627

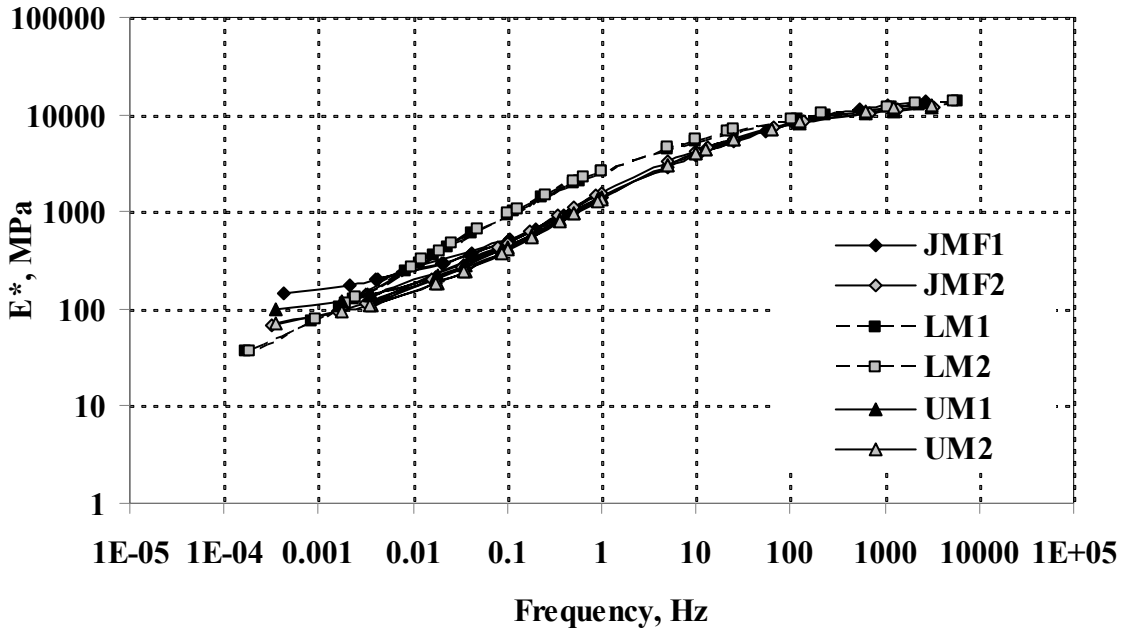

(f) Mix ID 5364

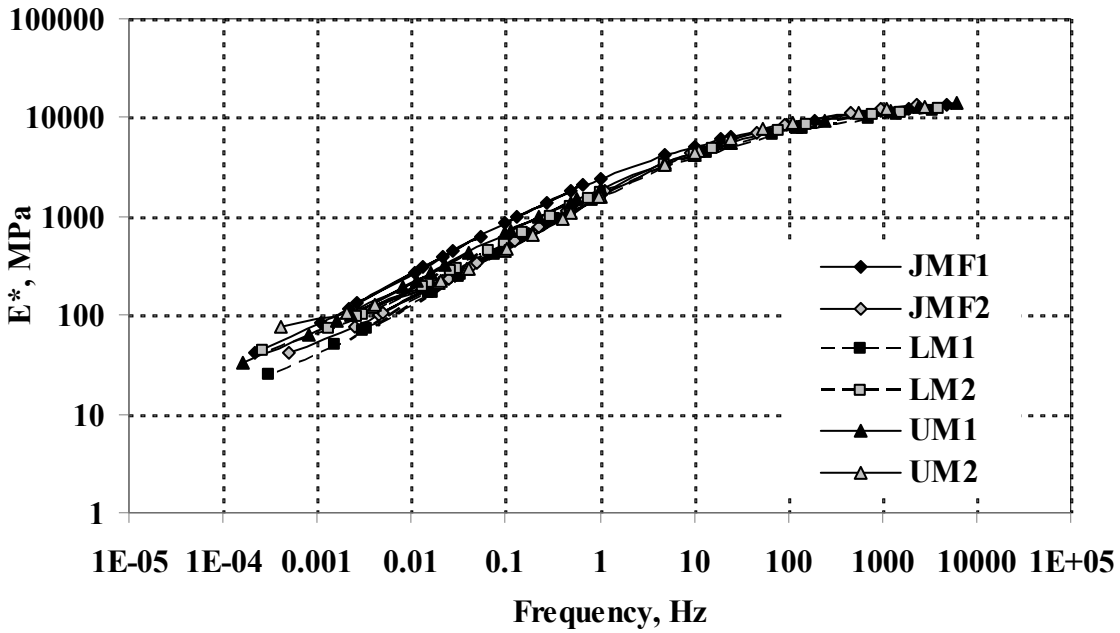

(f) Mix ID 5408

Fig. A2.1. Master curves of JMF and modified mixes

APPENDIX 3

Table A3.1. Traffic input data

Project	5381	5295	5192	5373	5627	5364	5408
SR	512	99	99	82	17	14	240
Location	Tacoma	Seattle	Tacoma	Yakima	Moses lake	Vancouver	Richland
Construction year	1998	1995	1998	1998	1999	1999	1998
Design life (years)				20			
Initial two-way AADTT	3701	900	1409	2181	1067	3473	1301
Number of lanes in design direction	4	6	4	4	2	4	6
Percent of trucks in design direction (%)	50	50	50	50	50	50	50
Percent of trucks in design lane (%)	90	70	90	90	100	90	70
Operational speed (mph)	60	40	50	60	60	60	55
Growth function				Compound growth			
Growth rate (%)	1.8	1.5	4.4	3.3	2.3	3.0	2.6

Table A3.2. Pavement structural layers used in the MEPDG analysis

Project	Layer	Material	Thickness (in)
5381	1	ACP CL 12.5 mm; PG 58-22 binder	1.8
	2	ACP CL B; AC-20	7.92
	3	Crushed stone granular base (compacted)	7.2
	4	Gravelly silty sand subgrade (compacted); A-2-4	Semi-infinite
5192	1	ACP CL 12.5 mm; PG 64-22 binder	1.8
	2	ACP CL B; AC-20	6
	3	Cement Stabilized (PCCP equivalent)	6.96
	4	Crushed stone granular base (compacted)	6
	5	Gravelly silty sand subgrade (compacted); A-2-4	Semi-infinite
5295	1	ACP CL 12.5 mm; PG 70-22 binder	1.8
		Grinding	-1.8
	2	ACP CL B; AC-20	2.16
	3	Cement stabilized base layer (PCCP equivalent)	9
	4	Crushed stone granular base (compacted)	6
	5	Gravelly silty sand subgrade (compacted); A-1-b	Semi-infinite
5373	1	ACP CL 19 mm; PG 70-28 binder	2.4
		Grinding	-1.44
	2	ACP CL A; AC-20	5.16
	4	Crushed stone granular base (compacted)	8.04
	5	Silt subgrade (compacted); A-4	Semi-infinite
5627	1	ACP CL 19 mm; PG 64-28 binder	3.6
	2	ACP CL B; AC-20	5.52
	3	Crushed stone granular base	7.44
	4	Gravelly silt subgrade	Semi-infinite
5364	1	ACP CL 12.5 mm; PG 58-22 binder	1.8
	2	ACP CL A; AC-20 binder	3
	3	Cement stabilized base layer (PCCP equivalent)	8.04
	4	Crushed stone granular base (compacted)	10.08
	5	Silty sand subgrade (compacted); A-2-4	Semi-infinite
5408	1	ACP CL 12.5 mm; PG 64-28 binder	2.4
		Grinding	-0.72
	2	ACP CL B; AC-20 binder	5.16
	3	Crushed stone granular base (compacted)	11.04
	4	Subgrade (compacted); A-2-4	Semi-infinite

Table A3.3. Existing asphalt layer material properties

Cumulative % retained 3/4" sieve	0
Cumulative % retained 3/8" sieve	15
Cumulative retained #4 sieve	20
% passing #200 sieve	3
Air voids, %	4
Total unit weight, pcf	145
Poisson's ratio	0.35
Thermal conductivity, BTU/hr-ft-F°	0.67[1]
Heat capacity, BTU/lb-F°	0.23[1]

[1] Default values in the software

Table A3.4. Level 1 predicted distress

Mix		IRI (in/mi)	AC Rutting (in)	Longitudinal Cracking (ft/mi)	Alligator Cracking (%)
5381	JMF1	79.8	0.097	2.49	0.0208
	JMF2	75.6	0.035	0	0.0006
	LM1	81.2	0.102	1.71	0.0237
	LM2	81	0.097	1.38	0.0226
	UM1	81.4	0.105	2.22	0.024
	UM2	81.4	0.106	2.99	0.0229
5295	JMF1	77.6	0.085	11.8	0
	JMF2	77.5	0.084	5.62	0
	LM1	77.6	0.086	7.86	0
	LM2	77.5	0.086	10.2	0
	UM1	77.5	0.085	8.22	0
	UM2	77.4	0.085	5.08	0
5192	JMF1	75.7	0.039	25.2	0.0096
	JMF2	81.4	0.043	0.0074	0.0074
	LM1	82.1	0.06	0.0076	0.0076
	LM2	81.4	0.042	0.0085	0.0085
	UM1	81.6	0.048	0.0084	0.0084
	UM2	75.6	0.038	0.009	0.009
5373	JMF1	97.3	0.141	12.3	0.0032
	JMF2	97.9	0.145	30.3	0.0044
	LM1	98.2	0.154	32	0.0037
	LM2	97.8	0.148	17	0.0028
	UM1	98.5	0.153	40.3	0.0023
	UM2	98.7	0.163	38.8	0.0023
5627	JMF1	97.8	0.057	0.8	0.0141
	JMF2	97.8	0.3	0.71	0.0139
	LM1	98.7	0.075	2.84	0.0164
	LM2	97.6	0.055	0.2	0.0136
	UM1	97.7	0.056	0.28	0.0135
	UM2	97.5	0.055	0.21	0.0126
5364	JMF1	87.1	0.261	14.7	0
	JMF2	87.1	0.258	17.4	0
	LM1	86.7	0.25	24.3	0
	LM2	86.6	0.249	23.6	0
	UM1	87.2	0.26	23.7	0
	UM2	87.1	0.26	15.5	0
5408	JMF1	101.8	0.166	27.7	0.0063
	JMF2	102.1	0.173	27.7	0.0054
	LM1	102.9	0.191	49.7	0.0043
	LM2	102.8	0.188	43.8	0.0044
	UM1	102.8	0.19	26.5	0.004
	UM2	102.4	0.18	33.4	0.0053

Table A3.5. Level 3 predicted distress

Mix		IRI (in/mi)	AC Rutting (in)	Longitudinal Cracking (ft/mi)	Alligator Cracking (%)
5381	JMF1	84.6	0.175	21	0.0324
	JMF2	84.1	0.163	8.57	0.0314
	LM1	84.6	0.176	12.5	0.0326
	LM2	84.6	0.176	13.7	0.0327
	UM1	84.1	0.163	12.3	0.0313
	UM2	84.3	0.169	18	0.0318
5295	JMF1	78	0.095	11.3	0
	JMF2	77.9	0.094	6.08	0
	LM1	78.1	0.096	8.46	0
	LM2	78.1	0.097	12.6	0
	UM1	77.9	0.094	8.17	0
	UM2	77.9	0.093	6.23	0
5192	JMF1	83.2	0.087	29	0.0055
	JMF2	83.1	0.086	25.3	0.0052
	LM1	83.3	0.091	38.6	0.0061
	LM2	83.3	0.091	38.6	0.0061
	UM1	83.1	0.085	32.5	0.0063
	UM2	83	0.083	24.1	0.0053
5373	JMF1	105.6	0.185	46.1	0.0003
	JMF2	106.1	0.194	109	0.0002
	LM1	106.5	0.201	118	0.0001
	LM2	106.1	0.195	60.6	0.0002
	UM1	105.9	0.189	93.9	0.0003
	UM2	105.8	0.189	87.5	0.0003
5627	JMF1	101.7	0.142	6.79	0.0201
	JMF2	101.7	0.141	6.33	0.02
	LM1	102.8	0.167	17.7	0.0218
	LM2	102.9	0.168	16.1	0.022
	UM1	100.9	0.125	2.21	0.0188
	UM2	100.8	0.123	1.88	0.0187
5364	JMF1	82.9	0.19	11.3	0.0018
	JMF2	88.6	0.296	14.7	0
	LM1	89.2	0.309	26.4	0
	LM2	89.2	0.309	26.4	0
	UM1	88.6	0.294	18.8	0
	UM2	88.4	0.291	13.1	0
5408	JMF1	106.1	0.262	82	0.0001
	JMF2	106	0.261	76.8	0.0001
	LM1	107.2	0.287	131	0.0001
	LM2	107.1	0.286	123	0.0001
	UM1	105.8	0.255	67.7	0.0002
	UM2	105.9	0.258	82.1	0.0002